Journal of Mathematical Biology (2020) 80:1617–1653
https://doi.org/10.1007/s00285-020-01475-0

Mathematical Biology

Dynamics of unidirectionally-coupled ring neural network with discrete and distributed delays

Bootan Rahman[1] · Yuliya N. Kyrychko[2] · Konstantin B. Blyuss[2]

Received: 18 June 2019 / Revised: 13 January 2020 / Published online: 30 January 2020

Abstract
In this paper, we consider a ring neural network with one-way distributed-delay coupling between the neurons and a discrete delayed self-feedback. In the general case of the distribution kernels, we are able to find a subset of the amplitude death regions depending on even (odd) number of neurons in the network. Furthermore, in order to show the full region of the amplitude death, we use particular delay distributions, including Dirac delta function and gamma distribution. Stability conditions for the trivial steady state are found in parameter spaces consisting of the synaptic weight of the self-feedback and the coupling strength between the neurons, as well as the delayed self-feedback and the coupling strength between the neurons. It is shown that both Hopf and steady-state bifurcations may occur when the steady state loses stability. We also perform numerical simulations of the fully nonlinear system to confirm theoretical findings.

Keywords Neural network · Stability · Discrete and distributed time delays · Weak gamma distributions

Mathematics Subject Classification 92B20 · 74H55 · 74H60

1 Introduction

Modern studies of neural networks have continued to develop some of the earlier research, such as the work done by Hopfield (1984), where he proposed a simple method of constructing a neural network model. That model, in which the linear circuit of each individual neuron consisted of a capacitor and a resistor, was capable

✉ Bootan Rahman
bootan.rahman@ukh.edu.krd

1 Mathematics Unit, School of Science and Engineering, University of Kurdistan Hewlêr (UKH), Erbil, Kurdistan Region, Iraq

2 Department of Mathematics, University of Sussex, Falmer, Brighton BN1 9QH, UK

of simulating the development of human memory. Hopfield went further and showed that through these electrical components, the connection between these neurons can be described by a nonlinear sigmoidal activation function. This profound realisation subsequently inspired the development of an entire field where electric circuit type models are used to study different problems, such as linear programming, signal processing, optimisation, associative memory and pattern recognition (Ahmadkhanlou and Adeli 2005; Amari and Cichocki 1998; Forti and Tesi 1995; Plaza et al. 2009; Zeng et al. 2008). Such applications heavily rely on underling dynamical behaviour, and therefore, the analysis of such dynamical effects as amplitude death, oscillation death, full and/or partial synchronization, clustering, localized pattern formation, and chimera states, is an important step for the practical design of realistic neural networks (Zakharova et al. 2013, 2017; Gjurchinovski et al. 2014, 2017).

It is important to note that by their very nature, neural networks inevitably incorporate time delays, since the transmission of information between the neurons is not instantaneous. Uncontrolled delays may degrade network performance and interfere with information processing by making equilibria unstable (Marcus and Westervelt 1989; Gopalsamy and Leung 1996; Pakdaman et al. 1998; Stépán 1989; Shayer and Campbell 2000; Gu et al. 2003; Erneux 2009; Gopalsamy 2013). In this respect, time delays usually play a destabilizing role when compared when compared to analogous models without time delays. Very recently, a number of important results have been obtained concerning the effects of discrete time delays on the dynamics of fuzzy (Xu et al. 2019c), fractional-order (Xu et al. 2019b), as well as BAM neural networks (Xu and Li 2019; Xu et al. 2019a). On should note that in many real situations the time delays are not constant; they may change over time and/or depend on system parameters (Gourley and So 2003; Feng 2010; Gjurchinovski and Urumov 2010). In the 1970s, some seminal papers, such as those by May (1973) and Cushing (1977) showed that in applications to biology, models with distributed delays are often more tractable and also more realistic than models with discrete delays. Since then, different types of distributed delays, typically represented by some distribution kernels, such as uniform or gamma distribution, have been studied in the context of modelling neural networks, where the presence of many parallel pathways with different axon sizes and lengths results in different distributions of transmission velocities, which can be studied using models with distributed time delays (Campbell 2007; Zhao 2004; Liao et al. 2001; Hutt and Zhang 2013; Han and Song 2012; Bernard et al. 2001; Kyrychko et al. 2011, 2013, 2014; Rahman et al. 2017a, b).

Recently, there has been a surge of interest in studying neural networks, often based on Hopfield-type models, with a combination of *both* discrete and distributed delays together. Biological justification for such an approach stems from an idea that when one considers neurons belonging to different parts of the brain, due to long-range (and possibly, multiple) connections between them, it is more appropriate to model their interactions using distributed delays (Song et al. 2009), whereas for neurons that are physically in close proximity of each other, discrete time delays provide a good representation, since variation in these delays is negligibly small compared to those in long-range connections (Rahman et al. 2015). Ruan and Filfil (2004) have studied the stability of steady-state solutions in a two-neuron model with both discrete and distributed delays, as well as a single feedback for each neuron, and discovered some interesting dynamical phenomena. Zhu and Huang (2007) have extended this model to a tri-neuron network with identical neurons and equivalent delays. They have shown that a Hopf bifurcation can occur when delays take certain critical values. Zhou et al. (2009) have investigated local stability of two neural networks with discrete and distributed delays. By taking the discrete time delay as a bifurcation parameter, they have found that the system undergoes a sequence of Hopf bifurcations. A number of other papers (Li and Hu 2011; Bi and Hu 2012; Du et al. 2013; Karaoğlu et al. 2016), have considered the dynamics of neural networks with discrete delays and different architectures. They found that the trivial steady state can loses its stability through a Hopf bifurcation, and identified the direction of Hopf bifurcation and the stability of bifurcating periodic solutions. Xu et al. (2014, 2019a) and Xu and Cao (2014) have investigated the stability and Hopf bifurcation in a class of neural networks with two neurons and in a high-dimension neural network. By using weak and strong distribution kernels, they have obtained conditions for the system keeping stable and undergoing the Hopf bifurcation, and then used DDE-BIFTOOL to confirm their analytical results. Feng (2014) has discussed the oscillatory behavior of the solutions for a three-node network model with discrete and distributed delays, using strong delay as a kernel distribution. Wang and Wang (2015) have analysed a model with two identical neurons with discrete and distributed delays. They found that the system can undergo the Hopf-pitchfork bifurcation if the neuron has negative self-inhibition and receives an external positive excitation from another neuron. Rahman et al. (2015) have analyzed a four-neuron model consisting of two subnetworks characterised by discrete delays within each subnetwork, and distributed delays between subnetworks. For a general delay distribution, they analytically obtained conditions that determine the stability of the trivial steady state, as well boundaries of steady-state and Hopf bifurcation of this steady state.

In order to make analytical progress, models based on Hopfield-type neural network are often characterise by low dimensionality, whereas actual biological networks are made up of an extremely large number of interconnected neurons. Naturally, increasing the size of the networks often leads to a much more complex theoretical analysis. One possible way to circumvent this complexity is to consider Hopfield-type neural networks with a simple architecture, such as a *ring network* (Baldi and Atiya 1994; Kaslik and Balint 2009; Jiang and Song 2014). In the specific context of neural networks, such models have been used to study a number of problems, such as gait, central pattern generation, and directional head movement, see Atiya and Baldi (1989), Canavier et al. (1997), Dror et al. (1999), Xie et al. (2002) and references therein. Moreover, ring networks have been identified in a variety of neural structures, such as hippocampus (Andersen et al. 1969), cerebellum (Eccles et al. 1967), and neocortex (Szentágothai 1975).

Baldi and Atiya (1994) have analysed the dynamics of the unidirectional ring neural model with time-delayed coupling, derived conditions for the onset of oscillations, and also determined periods of the bifurcating limit cycles. Campbell et al. (1999) modified this model by adding self-connected delay to the system. Yuan and Campbell (2004) developed the ring model further by considering a bidirectional delayed coupling between neurons. In the latter two papers, stability regions have been identified in the parameter space of the sum of time delays and the product of the coupling strengths, and the authors showed the presence of both steady-state and Hopf bifurcations. Xu (2008) has explored the dynamics of a ring neural model with a delayed two-way coupling and delayed self-connection. Using the Lyapunov functional approach, the global asymptotic stability of the steady state was shown under delay-independent and delay-dependent criteria. It was also shown how the steady state can lose its stability through a Hopf bifurcation, resulting in periodic oscillations. Mitra et al. (2014) have analysed a model based on the system with delayed unidirectional ring topology with self-feedback in the specific case of the Mackey–Glass model. They have shown the occurrence of phenomena such as amplitude death and synchronisation in their model. Lai et al. (2016) have investigated multistability and bifurcations in a ring-like neural network with four units, including the cases of one-way delayed coupling and delayed self-coupling.

In this paper, we consider a Hopfield-type network of unidirectionally coupled neurons with a discrete delayed self-feedback, and each ith neuron receiving a distributed

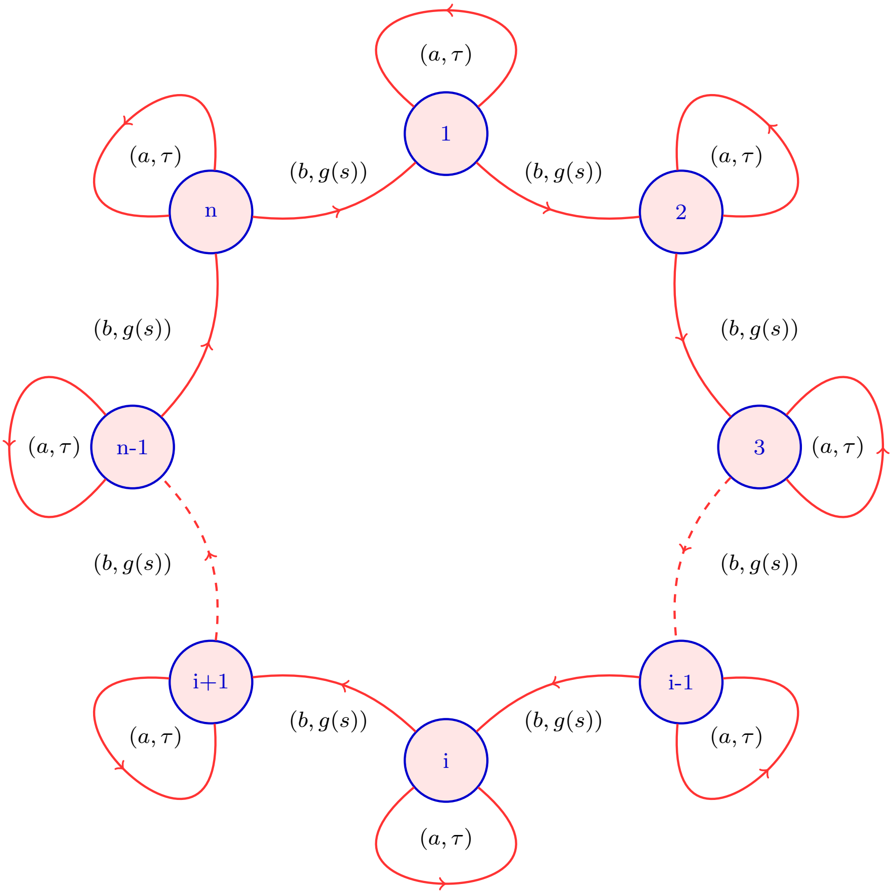

Fig. 1 Schematic sketch of the unidirectionally-coupled ring neural model with self-coupling described by the system (1)

delay signal from the $(i-1)$th neuron, as shown in Fig. 1. The model can be written in the form

$$\dot{u}_i(t) = -\kappa u_i(t) + af(u_i(t-\tau)) + b\int_0^\infty g(s)f(u_j(t-s))ds, \tag{1}$$

where $i = 1, 2, \ldots, n$ and

$$j = \begin{cases} n & \text{for } i = 1, \\ i & \text{for } i = 2, \ldots, n, \end{cases}$$

$\kappa > 0$, u_i denotes the voltage of the ith neuron, a is the synaptic weight of self-feedback, and b denotes the coupling strength of the neuron's connection, which can be positive or negative. We assume that a neuron has a delayed self-feedback input represented by a discrete time delay, and the transmission delays between neurons are characterised by a distribution kernel $g(\cdot)$.

The transfer function $f : \mathbb{R} \to \mathbb{R}$ is assumed to be sigmoid and in $\mathcal{C}^1$. For the local stability analysis, we only require $f(0) = 0$, $f'(0) \neq 0$, and will use a particular choice of $f(\cdot) = \tanh(\cdot)$ in the numerical simulations.

Without loss of generality, the distribution kernel $g(\cdot)$ is assumed to be normalised to unity and positive-definite, that is

$$\int_0^\infty g(s)ds = 1, \quad g(s) \geq 0.$$

In the case of the distribution kernel being a Dirac delta function, i.e. $g(s) = \delta(s-\sigma)$, the last term of the system (1) reduces to $bf(u(t-\sigma))$, which converts it to a unidirectionally-coupled ring neural system with discrete time delays in both self-feedback, and in the connection between the neurons.

The outline of the paper is as follows. In Sect. 2 we perform stability analysis of the trivial steady state of the system by looking at the characteristic equation for a generic delay distribution, and derive explicit conditions for stability in terms of system parameters. Sections 3 and 4 extend these general result to two specific delays distributions, namely, Dirac delta and weak gamma distributions. For both of these distributions we find conditions for stability of the trivial steady state, and fully identify boundaries of stability regions. In Sect. 5 we complement these analytical results by numerical stability analysis and simulations that illustrate different types of dynamical behaviours that can be exhibited by the model. Finally, Sect. 6 contains a discussion of results and open problems.

2 Stability analysis

Under assumption $f(0) = 0$, the system (1) always possesses a trivial steady state $(u_1, u_2, \ldots, u_n) = (0, 0, \ldots, 0)$. Linearising the system (1) near this trivial steady state gives

$$\dot{\mathbf{u}}(t) = -\kappa I\mathbf{u}(t) + \alpha I\mathbf{u}(t-\tau) + \beta M \int_0^\infty g(s)\mathbf{u}(t-s)ds, \tag{2}$$

where $\mathbf{u} = (u_1, u_2, \ldots, u_n)$, I is an $n \times n$ identity matrix, and M is given by

$$M = \begin{pmatrix} 0 & 0 & 0 & \cdots & 0 & 1 \\ 1 & 0 & 0 & \cdots & 0 & 0 \\ 0 & 1 & 0 & \cdots & 0 & 0 \\ \vdots & \vdots & \vdots & \cdots & \vdots & \vdots \\ 0 & 0 & 0 & \cdots & 1 & 0 \end{pmatrix}_{n\times n},$$

where $\alpha = af'(0) \neq 0$ and $\beta = bf'(0) \neq 0$. The characteristic equation can now be found as

$$\det[(\lambda + \kappa - \alpha e^{-\lambda\tau})I - \beta M\widehat{G}(\lambda)] = 0,$$

where

$$\widehat{G}(\lambda) = \int_0^\infty e^{-\lambda s} g(s)ds,$$

is the Laplace transform of the function $g(\cdot)$. The characteristic equation has the explicit form

$$(\lambda + \kappa - \alpha e^{-\lambda\tau})^n = (\beta\widehat{G}(\lambda))^n, \tag{3}$$

which can be equivalently written as

$$\Delta(\tau, \lambda) = 0, \tag{4}$$

with

$$\Delta(\tau, \lambda) = \begin{cases} \Delta_E(\tau, \lambda), & \text{if } n \text{ is even,} \\ \Delta_O(\tau, \lambda), & \text{if } n \text{ is odd,} \end{cases} \tag{5}$$

where $\Delta_E(\tau, \lambda)$ and $\Delta_O(\tau, \lambda)$ are

$$\Delta_E(\tau, \lambda) = \lambda + \kappa - \alpha e^{-\lambda\tau} \pm \beta\widehat{G}(\lambda) = 0 \tag{6}$$

and

$$\Delta_O(\tau, \lambda) = \lambda + \kappa - \alpha e^{-\lambda\tau} - \beta\widehat{G}(\lambda) = 0 \tag{7}$$

for even and odd n, respectively.

Lemma 1 $\lambda = 0$ *is a solution of the characteristic Eq.* (4) *if and only if* $|\beta| = \kappa - \alpha$ *when* n *is even, and* $\beta = \kappa - \alpha$ *when* n *odd.*

Proof From the characteristic Eqs. (6) and (7), computing $\widehat{G}(\lambda)$ at $\lambda = 0$ yields

$$\widehat{G}(0) = \int_0^{\infty} g(s)ds = 1.$$

Substituting this into $\Delta(\tau, 0) = 0$ given in (6), one has

$$\kappa - \alpha \pm \beta = 0,$$

and substituting it into (7) yields

$$\kappa - \alpha - \beta = 0,$$

which completes the proof. □

Lemma 2 *Let $|\beta| = \kappa - \alpha$ when n is even, and $\beta = \kappa - \alpha$ when n is odd. If the condition $E \neq \frac{\alpha\tau+1}{\alpha-\kappa}$ holds, where $E = \int_0^{\infty} sg(s)ds > 0$ is the mean time delay, then $\lambda = 0$ is a simple root of the characteristic Eq. (4).*

Proof Recall from Lemma 1 that if the condition $|\beta| = \kappa - \alpha$ holds when n is even, or the condition $\beta = \kappa - \alpha$ holds when n is odd, $\lambda = 0$ is a root of the characteristic Eq. (4). In order to determine the multiplicity of $\lambda = 0$, we compute implicit derivative of characteristic Eqs. (6) and (7) with respect to λ. When n is even, this gives

$$\frac{d\Delta_E}{d\lambda} = 1 + \alpha\tau e^{-\lambda\tau} \mp \beta \int_0^{\infty} se^{\lambda s} g(s)ds,$$

and when n is odd, one has

$$\frac{d\Delta_O}{d\lambda} = 1 + \alpha\tau e^{-\lambda\tau} + \beta \int_0^{\infty} se^{\lambda s} g(s)ds.$$

Recalling that $|\beta| = \kappa - \alpha$ when n is even, and $\beta = \kappa - \alpha$ when n is odd, and calculating the derivative at $\lambda = 0$, gives

$$\left.\frac{d\Delta}{d\lambda}\right|_{\lambda=0} = 1 + \alpha\tau + (\kappa - \alpha)E.$$

From the last expression, it is clear that if the condition $E \neq \frac{\alpha\tau+1}{\alpha-\kappa}$ is satisfied, then $\Delta(\tau, 0) \neq 0$, implying that $\lambda = 0$ is a simple root of the characteristic Eq. (4). □

It is well known that the trivial steady state $(u_1, u_2, \dots, u_n) = (0, 0, \dots, 0)$ is asymptotically stable if and only if all roots of the characteristic Eqs. (6) and (7) have negative real parts. We have the following result in a general case of the distribution kernel when all roots of the characteristic Eqs. (6) and (7) have negative real parts.

Theorem 1 *If the parameters of system (2) satisfy the condition $|\beta| < \kappa - |\alpha|$, the trivial solution of (1) is asymptotically stable for any distribution kernel and any $\tau \geq 0$.*

Proof Let $\lambda = \mu + i\omega$. Substituting this into the characteristic Eq. (6) and separating real and imaginary parts gives

$$\begin{aligned} \text{Re}[\Delta(\tau;\mu,\omega)] &= \mu + \kappa - \alpha e^{-\mu\tau}\cos(\omega\tau) \pm \beta \int_0^\infty e^{-\mu s}\cos(\omega s)g(s)ds, \\ \text{Im}[\Delta(\tau;\mu,\omega)] &= \omega + \alpha e^{-\mu\tau}\sin(\omega\tau) \mp \beta \int_0^\infty e^{-\mu s}\sin(\omega s)g(s)ds. \end{aligned} \tag{8}$$

The real part in (8) satisfies

$$\begin{aligned} \text{Re}[\Delta(\tau;\mu,\omega)] &\geq \mu + \kappa - |\alpha|e^{-\mu\tau} - |\beta| \\ &\quad\times \int_0^\infty e^{-\mu s}g(s)ds \geq R(\mu) = \mu + \kappa - |\alpha| - |\beta|. \end{aligned} \tag{9}$$

Since $|\beta| < \kappa - |\alpha|$, we now have $R(\mu) > 0$ for all $\mu \geq 0$, which implies from (9) that $\text{Re}[\Delta(\tau;\mu,\omega)] > 0$ for all $\mu \geq 0$. This means that any $\lambda = \mu + i\omega$ with $\mu \geq 0$ cannot be a root of the characteristic Eq. (6), which implies that all roots of this equation have a negative real part. The proof works in exactly the same way for the characteristic Eq. (7). □

Next, we are going to determine a region, where the trivial steady state is unstable for any distribution kernel $g(s)$ and $\tau \geq 0$.

Theorem 2 *The characteristic Eq.* (4) *has a root with a positive real part for any distribution kernel* $g(s)$ *and any* $\tau \geq 0$ *if one of the following conditions is satisfied: (i)* $|\beta| > \kappa - \alpha$ *when n is even, or* $\beta > \kappa - \alpha$ *when n is odd; or (ii)* $\alpha > \kappa$.

Proof Substituting $\lambda = 0$ into Eqs. (6) and (7) gives, respectively,

$$\Delta_E(\tau, 0) = \kappa - \alpha \pm \beta,$$

and

$$\Delta_O(\tau, 0) = \kappa - \alpha - \beta.$$

The assumption $|\beta| > \kappa - \alpha$ when n is even, or $\beta > \kappa - \alpha$ when n is odd, implies that $\Delta_E(\tau, 0) < 0$ and $\Delta_O(\tau, 0) < 0$, respectively. If the condition (ii) holds, then $\Delta_{E^-}(\tau, 0) = \kappa - \alpha - \beta < 0$ for $\beta \geq 0$, $\Delta_{E^+}(\tau, 0) = \kappa - \alpha + \beta < 0$ for $\beta \leq 0$ and $\Delta_O(\tau, 0) = \kappa - \alpha - \beta < 0$. On the other hand,

$$\lim_{\lambda\to\infty} \Delta_E(\tau,\lambda) = \infty, \qquad \lim_{\lambda\to\infty} \Delta_O(\tau,\lambda) = \infty.$$

Since $\Delta_E(\tau,\lambda)$ and $\Delta_O(\tau,\lambda)$ are continuous functions of λ, there exists $\lambda^* > 0$ such that $\Delta_E(\tau,\lambda^*) = 0$ and $\Delta_O(\tau,\lambda^*) = 0$ for any $\tau \geq 0$, and $|\beta| > \kappa - \alpha$ or $\beta > \kappa - \alpha$, respectively. Thus, the characteristic Eqs. (6) and (7) have a real positive root, which completes the proof. □

So far, we have been derived stability results for a general delay-distributed kernel. Figure 2 shows the shaded diamond-shaped domain in the (α, β) plane plane, where

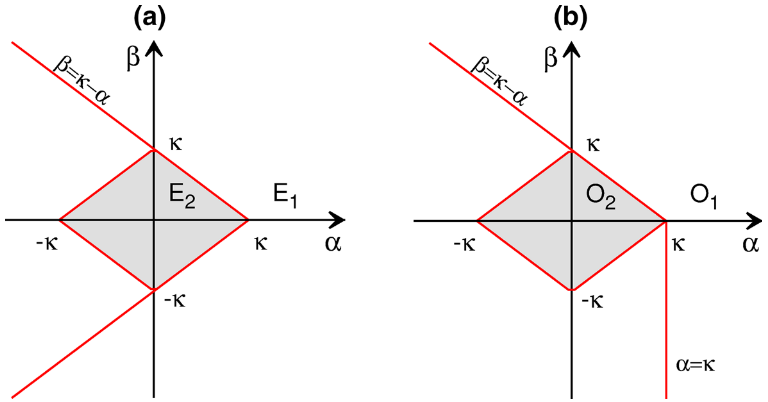

Fig. 2 Stability region of the trivial steady state of the system (1) in the parameter plane (α, β) for a general distribution kernel. The steady state is unstable in the region (E_1) (respectively, (O_1)), and asymptotically stable in the region (E_2) (respectively, (O_2) when n is even (**a**), or odd (**b**)

the trivial steady state is stable whenever the condition $|\beta| < \kappa - |\alpha|$ holds. The size of the diamond depends on the parameter κ for both even and odd n, as indicated in Theorem 1. From Theorem 2, it follows that it is impossible to stabilise the unstable trivial steady state in the regions E_1 in Fig. 2a and O_1 in Fig. 2b, if the parameters satisfy $|\beta| > \kappa - \alpha$ for even number of neurons, or if $\beta > \kappa - \alpha$ and $\alpha > \kappa$ for odd number of neurons.

Theorem 3 *When n is even, on the lines $|\beta| = \kappa - \alpha$, if $\tau < [(\alpha - \kappa)E - 1]/\alpha$, the trivial steady state becomes stable as β crosses the line $\beta = \kappa - \alpha$ decreasingly, or the line $\beta = -(\kappa - \alpha)$ increasingly, where $E = \int_0^\infty sg(s)ds > 0$ is the mean time delay.*

Proof Recall that the lines with $\lambda = 0$ are defined by the zero roots of $\Delta_E(\tau, \lambda) = 0$. Differentiating $\Delta_E(\tau, \lambda) = 0$ with respect to β, we obtain

$$\begin{aligned}\frac{d\mathrm{Re}(\lambda)}{d\beta} &= \mathrm{Re}\left(\frac{\pm\int_0^\infty g(s)e^{-\lambda s}ds}{1+\alpha\tau e^{-\lambda\tau} \mp \beta\int_0^\infty se^{-\lambda s}g(s)ds}\right)\\ &= \mathrm{Re}\left(\frac{\pm\widehat{G}(\lambda)}{1+\alpha\tau e^{-\lambda\tau} \mp \beta\int_0^\infty se^{-\lambda s}g(s)ds}\right).\end{aligned}$$

Evaluating this at $|\beta| = \kappa - \alpha$ and $\lambda = 0$, we have

$$\left.\frac{d\mathrm{Re}(0)}{d\beta}\right|_{|\beta|=\kappa-\alpha} = \pm\frac{1}{1+\alpha\tau+(\kappa-\alpha)E}. \tag{10}$$

Hence, $\left.\frac{d\mathrm{Re}(0)}{d\beta}\right|_{|\beta|=\kappa-\alpha} \lessgtr 0$, provided $\tau < [(\alpha - \kappa)E - 1]/\alpha$, and the trivial steady state becomes stable as β decreases through the line $\beta = \kappa - \alpha$ and increases through the line $\beta = -(\kappa - \alpha)$, which completes the proof. □

Theorem 4 *When n is odd, on the line $\beta = \kappa - \alpha$, $\beta > 0$, if $\tau < [(\alpha - \kappa)E - 1]/\alpha$, the trivial steady state becomes stable as β crosses the line $\beta = \kappa - \alpha$ decreasingly, where $E = \int_0^\infty sg(s)ds > 0$ is the mean time delay.*

Proof Recall that the $\lambda = 0$ line is defined by the zero roots of $\Delta_O(\tau, \lambda) = 0$. Differentiating $\Delta_O(\tau, \lambda) = 0$ with respect to β, yields

$$\begin{aligned}\frac{d\mathrm{Re}(\lambda)}{d\beta} &= \mathrm{Re}\left(\frac{\int_0^\infty g(s)e^{-\lambda s}ds}{1 + \alpha\tau e^{-\lambda\tau} + \beta\int_0^\infty se^{-\lambda s}g(s)ds}\right)\\ &= \mathrm{Re}\left(\frac{\widehat{G}(\lambda)}{1 + \alpha\tau e^{-\lambda\tau} + \beta\int_0^\infty se^{-\lambda s}g(s)ds}\right).\end{aligned}$$

Evaluating this at $\beta = \kappa - \alpha$ and $\lambda = 0$ yields

$$\left.\frac{d\mathrm{Re}(0)}{d\beta}\right|_{\beta=\kappa-\alpha} = \frac{1}{1 + \alpha\tau + (\kappa - \alpha)E}. \tag{11}$$

If $\tau < [(\alpha - \kappa)E - 1]/\alpha$, this implies that $\left.\frac{d\mathrm{Re}(0)}{d\beta}\right|_{\beta=\kappa-\alpha} < 0$, and, hence, the trivial steady state becomes stable as β decreases through the line $\beta = \kappa - \alpha$. This completes the proof. □

Remark 1 From Theorem 3, if $0 \le \alpha \le \kappa$, then the sign of $d\mathrm{Re}(0)/d\beta$ in (10) is fully determined by β and does not depend on the distribution kernel or the time delay $\tau \ge 0$. Thus, the trivial steady state loses stability via a steady-state bifurcation when β increases through the line $\beta = \kappa - \alpha$, or decreases through the line $\beta = -(\kappa - \alpha)$.

Remark 2 From Theorem 4, if $0 \le \alpha \le \kappa$, then $d\mathrm{Re}(0)/d\beta > 0$ in (11) regardless of the distribution kernel and the time delay $\tau \ge 0$. Thus, the trivial steady state loses stability via a steady-state bifurcation when β increases through the line $\beta = \kappa - \alpha$.

Remark 3 For a fixed value of α and for any distribution kernel, if $|\alpha| < \kappa$, then $\beta \ne 0$ for any $\tau \ge 0$. Furthermore, if $|\alpha| > \kappa$, then there exists τ_0 such that $\beta = 0$ for $\tau = \tau_0$.

Proof In order to find τ when $\beta = 0$ in Remark 3, let us assume that $\beta = 0$ in both characteristic Eqs. (6) and (7), which gives

$$\lambda + \kappa - \alpha e^{-\lambda\tau} = 0. \tag{12}$$

Substituting $\lambda = i\omega$ with $\omega > 0$ into (12) and separating real and imaginary parts, we obtain

$$\kappa = \alpha\cos(\omega\tau), \qquad -\omega = \alpha\sin(\omega\tau). \tag{13}$$

It can be easily seen that the Eqs. (13) can only be satisfied, if $|\alpha| > \kappa$. Under this assumption, squaring and adding (13) gives an expression for the Hopf frequency ω

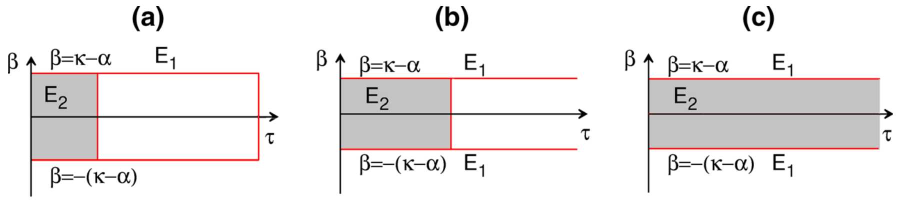

Fig. 3 Stability boundary of the trivial steady state of the system (1) in the (τ, β) parameter plane for a general distribution kernel when n is even. In the region E_1, the steady state is unstable, in the region E_2 it is asymptotically stable. **a** $\alpha < -\kappa$. **b** $-\kappa \leq \alpha < 0$. **c** $0 \leq \alpha \leq \kappa$

in the form $\omega = \sqrt{\alpha^2 - \kappa^2}$. Moreover, from the system (13), substituting ω, we can find the expressions for the time delay τ as follows

$$\tau \backsimeq \tau_j = \begin{cases} \dfrac{(2j+1)\pi - \cos^{-1}(\kappa/\alpha)}{\sqrt{\alpha^2 - \kappa^2}}, & \text{for } 0 < \kappa < \alpha, \\ \dfrac{2j\pi + \cos^{-1}(\kappa/\alpha)}{\sqrt{\alpha^2 - \kappa^2}}, & \text{for } \alpha < -\kappa < 0, \end{cases} \tag{14}$$

where $j = 0, 1, \ldots$. Since the trivial steady state is unstable for $\alpha > \kappa$, we are only interested in the case when $\alpha < -\kappa$. This simplifies the Eq. (14) as follows

$$\tau_0 = \frac{\cos^{-1}(\kappa/\alpha)}{\sqrt{\alpha^2 - \kappa^2}} \quad \text{for } \alpha < -\kappa < 0,$$

where $\cos^{-1}(\cdot)$ is the principal branch of the inverse $\cos(\cdot)$ function, which has the range $[0, \pi]$. □

Figure 3 illustrates a part of the stability region in (τ, β) plane for even n and a general distribution kernel $g(s)$. The shaded area E_2 in Fig. 3a, b indicates regions where the trivial steady state is stable when both conditions $\tau < [(\alpha - \kappa)E - 1]\alpha$ and $\alpha < 0$ are satisfied. This is in the full agreement with Theorem 3, which states that if β increases through the line $\beta = \kappa - \alpha$ or decreases through the line $\beta = -(\kappa - \alpha)$, the characteristic Eq. (5) has a real positive root. The closure in Fig. 3a reveals that for large enough values of the time delay τ and $\alpha < -\kappa$, the trivial steady state becomes unstable independently of the parameter β, as stated in Remark 3. In Fig. 3c, if $0 \leq \alpha \leq \kappa$, the trivial steady state can only lose its stability through the lines $|\beta| = \kappa - \alpha$. Finally, for $\alpha > \kappa$, the zero steady state is always unstable for $\tau \geq 0$, following the results of Theorem 2(ii).

Figure 4 shows stability regions for odd number of neurons and different values of α. For all the three cases, from Theorem 4 it follows that the trivial steady state becomes stable as β passes through the line $\beta = \kappa - \alpha$ decreasingly. The shaded area O_2 in Fig. 4a, b indicates the region where that the trivial steady state is stable, provided $\tau < [(\alpha - \kappa)E - 1]/\alpha$ and $\alpha < 0$. The shaded area O_2 in Fig. 4c is a stability region for $\alpha > 0$, as stated in Remark 2. For both even and odd number of neurons, Theorem 2(ii) shows that if $\alpha > \kappa$, the trivial steady state is always unstable

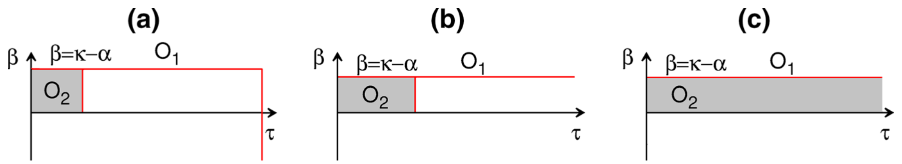

Fig. 4 Stability boundary of the trivial steady state of the system (1) in the (τ, β) parameter plane for a general distribution kernel when n is odd. In region O_1, the steady state is unstable, and in region O_2 it is asymptotically stable. **a** $\alpha < -\kappa$. **b** $-\kappa \le \alpha < 0$. **c** $0 \le \alpha \le \kappa$

independently of the time delay τ. It is noteworthy to mention that the trivial steady state undergoes a steady-state bifurcation through horizontal lines $|\beta| = \kappa - \alpha$ when n is even, and $\beta = \kappa - \alpha$ when n is odd, as illustrated in Figs. 3 and 4, and stated in Lemma 2.

Due to the complexity of the system, it is not possible to find the full stability region for a general distribution kernel. Therefore, we now consider specific delay kernels to make further analytical progress and to find complete stability regions for a trivial steady state.

3 Dirac delta function distribution

When the delay distribution kernel if chosen as a Dirac delta function, there are two possibilities. If $g(s) = \delta(s - \sigma)$, then the system (1) reduces to a system with two distinct discrete time delays. This case has been considered for a system of two neurons in Shayer and Campbell (2000), a three-neuron network in Yuan and Li (2010), a four-neuron system in Williams et al. (2013), and a ring network of n neurons in Campbell et al. (1999) and Mitra et al. (2014).

Let us instead consider the distribution kernel of the form $g(s) = \delta(s)$, i.e

$$\int_0^\infty f(\mathbf{u}(t - s))\delta(s)ds = f(\mathbf{u}(t)). \tag{15}$$

In this case, the linearised model (2) becomes a system with a discrete time delay only, and has the form

$$\dot{\mathbf{u}}(t) = (-\kappa I + \beta M)\mathbf{u}(t) + \alpha I\mathbf{u}(t - \tau), \tag{16}$$

where $\mathbf{u} = (u_1, u_2, \ldots, u_n)$, I is an $n \times n$ identity matrix, and M is defined in (2). The corresponding characteristic equations for even and odd n, respectively, are

$$\Delta_E(\tau, \lambda) = \lambda + \kappa \pm \beta - \alpha e^{-\lambda\tau} = 0, \tag{17}$$

and

$$\Delta_O(\tau, \lambda) = \lambda + \kappa - \beta - \alpha e^{-\lambda\tau} = 0. \tag{18}$$

In Sect. 2, we have analysed the characteristic equation for an arbitrary distribution kernel and obtained a subset of stability boundary in both (α, β) and (τ, β) parameter planes. We now consider the same parameter spaces to determine the complete stability region in the case $g(s) = \delta(s)$.

Theorem 5 *For the system* (1) *with delta distributed kernel* $g(s) = \delta(s)$ *and even n, the following holds.*

(i) *The trivial steady state is unstable if* $|\beta| > \kappa - \alpha$.
(ii) *The trivial steady state is asymptotically stable if* $|\beta| < \kappa - |\alpha|$.
(iii) *The trivial steady state is stable if* $\kappa + \alpha < |\beta| < \kappa - \alpha$ *and* $\tau \in [0, \tau_{even})$. *At* $\tau = \tau_{even}$, *the trivial steady state loses its stability via a Hopf bifurcation and becomes unstable for* $\tau > \tau_{even}$, *where* τ_{even} *is the first critical time delay given by* $\tau_{even} = \min\{\tau_0^-, \tau_0^+\}$, *with*

$$\tau_0^\pm = \frac{\cos^{-1}(\frac{\kappa\pm\beta}{\alpha})}{\sqrt{\alpha^2 - (\kappa \pm \beta)^2}}.$$

Proof Results (i) and (ii) immediately follow from Theorems 1 and 2 . In (iii), assume that condition $\kappa + \alpha < |\beta| < \kappa - \alpha$ is satisfied. First, for $\tau = 0$, the characteristic Eq. (17) becomes $\Delta_E(0, \lambda) = \lambda + \kappa \pm \beta - \alpha$, with the eigenvalues given as $\lambda^* = -(\kappa \pm \beta - \alpha)$. Since $|\beta| < \kappa - \alpha$, $\lambda^* < 0$, and, therefore, the trivial steady state is stable. Now, we consider the case when $\tau > 0$ and look for eigenvalues in the form $\lambda = i\omega$, $\omega > 0$. Substituting $\lambda = i\omega$ into (17), and separating real and imaginary parts, we get

$$\begin{aligned} &\kappa \pm \beta - \alpha \cos(\omega\tau) = 0, \\ &\omega + \alpha \sin(\omega\tau) = 0. \end{aligned} \tag{19}$$

Upon squaring and adding these two equations, one obtains

$$\omega^2 = \alpha^2 - (\kappa \pm \beta)^2, \tag{20}$$

and from the first equation of the system (19) it follows that

$$\tau_j^\pm = \begin{cases} \dfrac{(2j+1)\pi - \cos^{-1}\left(\frac{\kappa\pm\beta}{\alpha}\right)}{\sqrt{\alpha^2 - (\kappa \pm \beta)^2}} & \text{for } 0 < \kappa \pm \beta < \alpha, \\ \dfrac{2j\pi + \cos^{-1}\left(\frac{\kappa\pm\beta}{\alpha}\right)}{\sqrt{\alpha^2 - (\kappa \pm \beta)^2}} & \text{for } \alpha < -(\kappa \pm \beta) < 0. \end{cases} \tag{21}$$

Since $|\beta| < \kappa - \alpha$, the latter expression for $\tau_j^\pm$ becomes

$$\tau_j^\pm = \frac{\cos^{-1}(\frac{\kappa\pm\beta}{\alpha}) + 2j\pi}{\sqrt{\alpha^2 - (\kappa \pm \beta)^2}}, \tag{22}$$

where $j = 0, 1, 2, \ldots$.

To show that a Hopf bifurcation occurs at $\tau = \tau_{even}$, we note that solutions of Eq. (19) are pairs $(\tau_j^{\pm}, \omega)$, such that $\lambda = \pm i\omega$ are pairs of purely imaginary roots of (17) with $\tau = \tau_j^{\pm}$. Define

$$\tau_{even} = \min\{\tau_0^-, \tau_0^+\},$$

where τ_{even} is the first critical value of the time delay τ, for which the roots of Eq. (17) cross the imaginary axis. In order to determine the direction of the root crossing, we differentiate the characteristic Eq. (17) with respect to α:

$$\frac{d\lambda}{d\alpha} = \frac{e^{-\lambda\tau}}{1 + \alpha\tau e^{-\lambda\tau}} = \frac{1}{e^{\lambda\tau} + \alpha\tau}. \tag{23}$$

From (23) it follows that

$$\frac{d\mathrm{Re}(\lambda)}{d\alpha} = \frac{\alpha\tau + \cos(\omega\tau)}{(\alpha\tau + \cos(\omega\tau))^2 + (\sin(\omega\tau))^2}. \tag{24}$$

Using the first equation of (19), we obtain

$$\alpha\tau + \cos(\omega\tau) = \alpha\tau + \frac{\kappa \pm \beta}{\alpha} > \alpha\tau + \frac{\alpha}{\alpha} = \alpha\tau + 1,$$

which implies that $\alpha\tau + 1 < 0$ if $\alpha < -\frac{1}{\tau}$. This completes the proof. □

Theorem 6 *For the system* (1) *with delta distributed kernel* $g(s) = \delta(s)$ *and odd* n, *the following holds.*

(i) *The trivial steady state is unstable if* $\beta > \kappa - \alpha$ *and* $\alpha > \kappa$.
(ii) *The trivial steady state is asymptotically stable if* $|\beta| < \kappa - |\alpha|$.
(iii) *The trivial steady state is stable if* $\beta < \kappa - \alpha$, $\alpha < \kappa$ *and* $\tau \in [0, \tau_{odd})$, *a Hopf bifurcation occurs at* $\tau = \tau_{odd}$, *and the steady state is unstable for all* $\tau > \tau_{odd}$, *where* τ_{odd} *is the first critical time delay given by*

$$\tau_{odd} = \frac{\cos^{-1}(\frac{\kappa-\beta}{\alpha})}{\sqrt{\alpha^2 - (\kappa-\beta)^2}}.$$

Proof The proof of this theorem is similar to the proof of Theorem 5. In order to find τ_{odd}, we look for eigenvalues of the characteristic equation in the form $\lambda = i\omega$, substitute this into (17), and separating real and imaginary parts, we obtain

$$\begin{aligned} \kappa - \beta - \alpha\cos(\omega\tau) &= 0, \\ \omega + \alpha\sin(\omega\tau) &= 0. \end{aligned} \tag{25}$$

Squaring and adding these two equations yields

$$\omega^2 = \alpha^2 - (\kappa - \beta)^2, \tag{26}$$

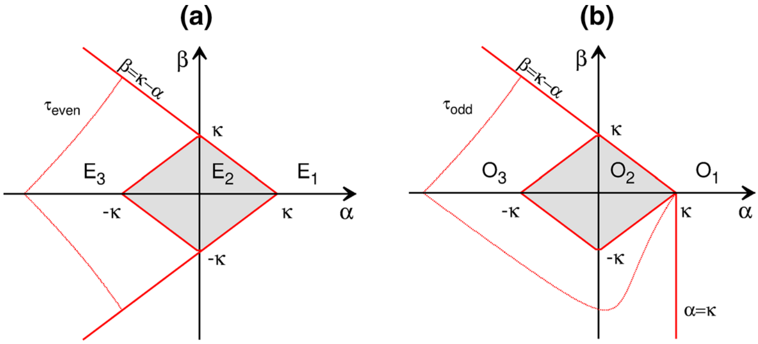

Fig. 5 Stability boundary of the trivial steady state of the system (1) with delta distribution kernel in (α, β) parameter space. When n is even (**a**)/odd (**b**), the trivial steady state is unstable in region E_1/O_1, asymptotically stable in region E_2/O_2, and stable in region E_3/O_3 when $\tau \in [0, \tau_{even})/[0, \tau_{odd})$

and from the first equation of the system (25), one obtains

$$\tau_j^- = \begin{cases} \dfrac{(2j+1)\pi - \cos^{-1}\left(\frac{\kappa-\beta}{\alpha}\right)}{\sqrt{\alpha^2 - (\kappa-\beta)^2}} & \text{for } 0 < \kappa - \beta < \alpha, \\ \dfrac{2j\pi + \cos^{-1}\left(\frac{\kappa-\beta}{\alpha}\right)}{\sqrt{\alpha^2 - (\kappa-\beta)^2}} & \text{for } \alpha < -(\kappa-\beta) < 0, \end{cases} \tag{27}$$

where $\tau_{odd} = \tau_0^-$ is the first critical time delay, when the trivial steady state loses its stability. The proof of transversality condition is analogous to the one in Theorem 5. This completes the proof. □

Theorems 5 and 6 give stability properties of the trivial steady state in (α, β) parameter space for Dirac delta delay distribution kernel $g(s) = \delta(s)$. When n is even, the stability region is bounded by lines $|\beta| = \kappa - \alpha$ to the left of the shaded diamond, and remains symmetric with respect to α-axis, as shown in Fig. 5a. Figure 5b shows the stability boundary for the case when n is odd. In this case, the region of stability is enlarged towards down and to the left of the shaded diamond, and unlike the case when n is even, the stability region becomes asymmetric around α-axis.

Next, we analyse stability properties of the trivial steady state of the system (2) in (τ, β) parameter plane.

Theorem 7 *For the system* (1) *with delta distributed kernel* $g(s) = \delta(s)$ *and even* n, *the following statements hold.*

(i) *For* $\alpha < 0$, *the trivial steady state is asymptotically stable if* $|\beta| < \kappa - \alpha$ *and* $\tau < -1/\alpha$. *When* β *is increased (decreased) through the line* $|\beta| = \kappa - \alpha$, *the trivial steady state loses its stability via a steady-state bifurcation. The trivial steady state is stable if* $|\beta| < \kappa - \alpha$ *and* $\tau \in [-1/\alpha, \tau_{even})$. *At* $\tau = \tau_{even}$, *the trivial steady state undergoes a Hopf bifurcation, and it is unstable for* $\tau > \tau_{even}$. *For* $\alpha < -\kappa$, *the trivial steady state is unstable independent of* β *for* $\tau > \tau_{odd} = \cos^{-1}(\kappa/\alpha)/\sqrt{\alpha^2 - \kappa^2}$.

(ii) *For* $0 \leq \alpha \leq \kappa$*, the trivial steady state is asymptotically stable if* $|\beta| < \kappa - \alpha$ *and unstable if* $|\beta| > \kappa - \alpha$*. When* β *is increased (decreased) through the line* $|\beta| = \kappa - \alpha$*, the trivial steady state undergoes a steady-state bifurcation, independently of the time delay* τ*.*

Proof Following stability results in the case of the general distribution kernel, as stated in Theorem 3 and Remark 1, we have proved the results in (i) and (ii) that are related to the appearance of the steady-state bifurcation. We have also shown that the trivial steady state is unstable independent of β in Remark 3 for $\alpha < -\kappa$. In order to show the occurrence of a Hopf bifurcation in (i) and (ii) when $\tau = \tau_{even}$, differentiating Eq. (17) implicitly with respect to τ, we find

$$\frac{d\lambda}{d\tau} = -\frac{\alpha e^{-\lambda\tau}}{1 + \alpha\tau e^{-\lambda\tau}}. \tag{28}$$

Substituting $\lambda = i\omega$ into (28) and taking real part, one has

$$\frac{d\mathrm{Re}(\lambda)}{d\tau} = -\frac{\alpha[1 + \alpha\tau\cos(\omega\tau)]}{(1 + \alpha\tau\cos(\omega\tau))^2 + (\alpha\tau\sin(\omega\tau))^2}. \tag{29}$$

Using the first equation of (19) yields

$$1 + \alpha\tau\cos(\omega\tau) = 1 + \tau(\kappa \pm \beta) > 1 + \tau\alpha,$$

which implies that $1+\tau\alpha > 0$ if $\tau > -1/\alpha$, and since $\alpha < 0$, we conclude that for $\tau = \tau_{even}$, there is a root $\lambda = \lambda(\tau) = \alpha(\tau) \pm i\omega(\tau)$ satisfying $\alpha(\tau_{even}) = 0,\ \omega(\tau_{even}) = \omega$ and $d\mathrm{Re}(\lambda)/d\tau\big|_{\tau=\tau_{even}} > 0$. This root crosses the imaginary axis at $\tau = \tau_{even}$ from left to right if $\tau > -1/\alpha$, which completes proof. □

Theorem 8 *For the system* (1) *with delta distributed kernel* $g(s) = \delta(s)$ *when n is odd, the following statements hold.*

(i) *For* $\alpha < 0$ *and* $\beta > 0$*, the trivial steady state is asymptotically stable if* $\beta < \kappa - \alpha$ *and* $\tau < -1/\alpha$*. When* β *increases through the line* $\beta = \kappa - \alpha$*, a steady-state bifurcation occurs. If* $\beta < \kappa - \alpha$*, the trivial steady state is stable if* $\tau \in [-1/\alpha, \tau_{odd})$*, unstable if* $\tau > \tau_{odd}$*, and undergoes a Hopf bifurcation at* $\tau = \tau_{odd}$*. For* $\alpha < 0$ *and* $\beta < 0$*, the trivial steady state is stable if* $\tau \in [0, \tau_{odd})$*, unstable if* $\tau > \tau_{odd}$*, and undergoes a Hopf bifurcation at* $\tau = \tau_{odd}$*. For* $\alpha < -\kappa$*, the trivial steady state is unstable independent of* β *for* $\tau > \tau_0 = \cos^{-1}(\kappa/\alpha)/\sqrt{\alpha^2 - \kappa^2}$*.*

(ii) *For* $0 \leq \alpha \leq \kappa$ *and* $\beta > 0$*, the trivial steady state is asymptotically stable if* $\beta < \kappa - \alpha$ *and loses stability via a steady-state bifurcation when* β *is increased through the line* $\beta = \kappa - \alpha$*, independently of the time delay* τ*. For* $0 < \alpha \leq \kappa$ *and* $\beta < 0$*, the trivial steady state undergoes a Hopf bifurcation at* $\tau = \tau_{odd}$*.*

Proof Similarly to the proof of Theorem 7, existence of the steady-state bifurcation follows directly from stability results for a general distribution kernel, as stated in Theorem 4 and Remarks 2 and 3 . In order to show the occurrence of a Hopf bifurcation

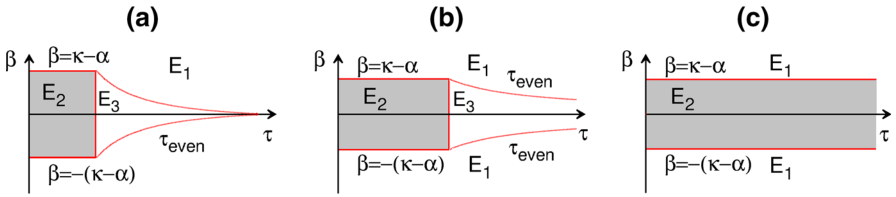

Fig. 6 Stability boundary of the trivial steady state of the system (1) with Dirac delta distributed kernel in (τ, β) parameter space when n is even. The trivial steady state is unstable in region E_1, asymptotically stable in region E_2, and stable in region E_3 for $\tau < \tau_{even}$. **a** $\alpha < -\kappa$. **b** $-\kappa \le \alpha < 0$. **c** $0 \le \alpha \le \kappa$

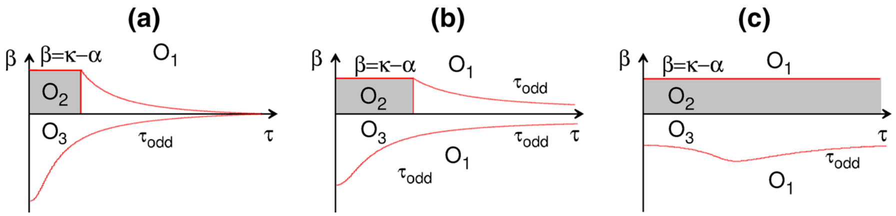

Fig. 7 Stability boundary of the trivial steady state of the system (1) with Dirac delta distributed kernel in the (τ, β) plane when n is odd. The trivial steady state is unstable in region O_1, asymptotically stable in region O_2, and stable in region O_3 for $\tau < \tau_{odd}$. **a** $\alpha < -\kappa$. **b** $-\kappa \le \alpha < 0$. **c** $0 \le \alpha \le \kappa$

in (i) and (ii), when $\tau = \tau_{even}$, we differentiate Eq. (18) implicitly with respect to τ to obtain

$$\frac{d\lambda}{d\tau} = -\frac{\alpha e^{-\lambda\tau}}{1 + \alpha\tau e^{-\lambda\tau}}, \tag{30}$$

which then gives

$$\frac{d\text{Re}(\lambda)}{d\tau} = \frac{-\alpha[1 + \alpha\tau\cos(\omega\tau)]}{(1 + \alpha\tau\cos(\omega\tau))^2 + (\alpha\tau\sin(\omega\tau))^2}. \tag{31}$$

For $\alpha < 0$ and $0 < \beta < \kappa - \alpha$, using the first Eq. of (25) we obtain $-\alpha[1 + \alpha\tau\cos(\omega\tau) = -\alpha[1 + \tau(\kappa - \beta)] > -\alpha(1 + \tau\alpha) > 0$ if $\tau > -\frac{1}{\alpha}$. For $\alpha < 0$ and $\beta < 0$, we have $1 + \alpha\tau\cos(\omega\tau) = 1 + \tau(\kappa - \beta) > 0$, which completes the proof. □

Theorems 7 and 8, illustrate the full stability region in (τ, β) parameter plane. For a Dirac delta distribution, the condition for a general distributed kernel $\tau < [(\kappa - \alpha)E - 1]/\alpha$ reduces to $\tau < -1/\alpha$, and the stability region has three different shapes in the parameter plane depending on values of other parameters. When n is even and $\alpha < 0$, as illustrated in Fig. 6a, b, the trivial steady state is asymptotically stable if $|\beta| < \kappa - \alpha$ and $\tau < -1/\alpha$, it is further stable for $\tau \in [-\frac{1}{\alpha}, \tau_{even})$, and undergoes a Hopf bifurcation at $\tau = \tau_{even}$. As we discussed in previous section and shown in Fig. 6a, if $\alpha < -\kappa$, for large enough values of τ the trivial steady state is unstable independently of β. When $0 \le \alpha \le \kappa$, as shown in Fig. 6c, there is no difference in stability regions between a delta function distribution and a general distribution. When n is odd, again it gives three boundary regions. The shape of stability regions when n is odd and $\beta > 0$ is the same as for the case when n is even. The asymmetry in stability regions arises when $\beta < 0$ for all three scenarios shown in Fig. 7.

4 Weak gamma distributed delay

Another commonly used delay distribution is the so-called Gamma distribution, which can be written as follows,

$$g(u) = \frac{u^{p-1}\gamma^p e^{-\gamma u}}{(p-1)!}, \tag{32}$$

where $\gamma,\ p \geq 0$ and p is integer. For $p = 1$ this is an exponential distribution, also called a *weak delay kernel*. Weak delay distribution has the mean delay

$$\tau_m = \int_0^\infty u g(u) du = \frac{p}{\gamma}, \tag{33}$$

and the variance

$$\sigma^2 = \int_0^\infty (u - \tau_m)^2 g(u) du = \frac{p}{\gamma^2}. \tag{34}$$

Laplace transform of the weak delay distribution kernel has the form

$$\hat{G}(\lambda) = \left(\frac{\gamma}{\lambda + \gamma}\right)^p. \tag{35}$$

Substituting this Laplace transform into Eqs. (6) and (7) shows that the the characteristic equation in this case becomes

$$\lambda^2 + p_1\lambda + p_2 + (q_1\lambda + q_2)e^{-\lambda\tau} = 0, \tag{36}$$

where

$$p_1 = \gamma + \kappa, \quad q_1 = -\alpha, \quad q_2 = -\alpha\gamma \quad p_2 = \begin{cases} (\kappa \pm \beta)\gamma & \text{if } n \text{ is even,} \\ (\kappa - \beta)\gamma & \text{if } n \text{ is odd.} \end{cases} \tag{37}$$

In order to determine the boundaries of stability of the trivial steady state of the system (1), we investigate the distribution of roots of characteristic Eq. (36), and more specifically, look for roots with zero real part. This can happen either when $\lambda = 0$, or when $\lambda = i\omega\,(\omega > 0)$. As was shown in Lemma 1 for any distribution kernel, $\lambda = 0$ is a solution of the characteristic Eq. (36) if and only if $|\beta| = \kappa - \alpha$ when n is even, and $\beta = \kappa - \alpha$ when n is odd. In order to find the complete boundaries of the stability region, we look consider a situation when the characteristic equation has a pair of purely imaginary roots. Substituting $\lambda = i\omega$ into Eq. (36) gives

$$-\omega^2 + p_1\omega i + p_2 + (q_1\omega i + q_2)(\cos(\omega\tau) - i\sin(\omega\tau) = 0. \tag{38}$$

Separating real and imaginary parts of this equation yields

$$\begin{cases} \omega^2 - p_2 = q_2 \cos(\omega\tau) + q_1\omega \sin(\omega\tau), \\ p_1\omega \qquad = q_2 \sin(\omega\tau) - q_1\omega \cos(\omega\tau). \end{cases} \tag{39}$$

Squaring and adding these two equations, one obtains a quartic equation

$$\omega^4 - (q_1^2 + 2p_2 - p_1^2)\omega^2 + p_2^2 - q_2^2 = 0, \tag{40}$$

whose solutions can be readily found as

$$\omega_\pm^2 = \frac{(q_1^2 + 2p_2 - p_1^2) \pm \sqrt{(q_1^2 + 2p_2 - p_1^2)^2 - 4(p_2^2 - q_2^2)}}{2}. \tag{41}$$

Let us define $\Phi = (q_1^2 + 2p_2 - p_1^2)^2 - 4(p_2^2 - q_2^2) < 0$. We now distinguish between the following cases:

(H1) $p_2^2 - q_2^2 > 0$ and $q_1^2 + 2p_2 - p_1^2 < 0$ or $\Phi < 0$. In this case, Eq. (40) has no real roots.

(H2) $p_2^2 - q_2^2 < 0$ or $q_1^2 + 2p_2 - p_1^2 > 0$ and $\Phi = 0$. In this case, Eq. (40) has one positive root ω_+ given by

$$\omega_+ = \frac{\sqrt{2}}{2}[q_1^2 + 2p_2 - p_1^2 + \sqrt{\Phi}]^{\frac{1}{2}}.$$

(H3) $p_2^2 - q_2^2 > 0$, $q_1^2 + 2p_2 - p_1^2 > 0$ and $\Phi > 0$. In this case, Eq. (40) has two positive roots $\omega_\pm = \frac{\sqrt{2}}{2}[q_1^2 + 2p_2 - p_1^2 \pm \sqrt{\Phi}]^{\frac{1}{2}}$.

If either of the hypotheses (H2) or (H3) holds, the characteristic Eq. (36) has purely imaginary roots for some $\tau = \tau_j^\pm$. To find these values of τ, we solve the system (39) for $\sin(\omega\tau)$ and $\cos(\omega\tau)$ and then divide those to obtain the following expressions for the critical time delays

$$\tau_j^\pm = \frac{1}{\omega_\pm}\left\{\tan^{-1}\left(-\frac{\omega_\pm(q_1\omega_\pm^2 + p_1q_2 - p_2q_1)}{p_1q_1\omega_\pm^2 - q_2\omega_\pm^2 + p_2q_2}\right) + j\pi\right\}, \qquad j = 0, 1, 2, \ldots. \tag{42}$$

Here we define

$$\tau_{weak} = \min\{\tau_0^-, \tau_0^+\}$$

as the first critical time delay. Note that when $\tau = 0$, the system (1) with gamma distribution (32) reduces to a system of ODEs with a characteristic equation

$$\lambda^2 + (p_1 + q_1)\lambda + p_2 + q_2 = 0. \tag{43}$$

Lemma 3 *Assume that (H4) $p_1 + q_1 > 0$ and $p_2 + q_2 > 0$. Then all roots of the Eq. (43) with $\tau = 0$ have negative real parts.*

Lemma 4 *Suppose that (H4) holds, and $\omega_\pm^2$ and $\tau_j^\pm$ are defined by Eqs. (41) and (42), respectively.*

(i) *If (H1) is satisfied, then there are no roots of Eq. (36) with positive real part for any $\tau \geq 0$.*
(ii) *If (H2) is satisfied, then there are no roots of Eq. (36) with positive real part for for $\tau \in [0, \tau_{weak})$, and there is a pair of simple purely imaginary roots $\pm i\omega_+$ at $\tau = \tau_{j^+}$.*
(iii) *If (H3) is satisfied, then there are no roots of Eq. (36) with positive real part for for $\tau \in [0, \tau_{weak})$, and there is a pair of simple purely imaginary roots $\pm i\omega_\pm$ at $\tau = \tau_j^\pm$, respectively.*

Under the hypothesis (H3), the characteristic Eq. (36) has two pairs of purely imaginary roots $i\omega_\pm$ with $\omega_+ > \omega_- > 0$ defined by (41). In order to establish whether stability of the trivial steady state actually changes as τ varies, we calculate the sign of the derivative of Re(λ) at the points where $\lambda(\tau)$ is purely imaginary.

Lemma 5 *The following transversality conditions are satisfied*

$$\left[\frac{dRe\{\lambda(\tau)\}}{d\tau}\right]_{\tau=\tau_j^+} > 0, \quad \left[\frac{dRe\{\lambda(\tau)\}}{d\tau}\right]_{\tau=\tau_j^-} < 0.$$

Proof Differentiating the characteristic Eq. (36) implicitly with respect to τ, we find

$$\left[\frac{d\lambda}{d\tau}\right]^{-1} = \frac{2\lambda + p_1 + q_1 e^{-\lambda\tau} - (q_1\lambda + q_2)\tau e^{-\lambda\tau}}{(q_1\lambda + q_2)\lambda e^{-\lambda\tau}} = \frac{(2\lambda + p_1)e^{\lambda\tau}}{(q_1\lambda + q_2)\lambda} + \frac{q_1}{(q_1\lambda + q_2)\lambda} - \frac{\tau}{\lambda}.$$

Now, we can compute

$$\begin{aligned}
&\left[\frac{d\mathrm{Re}\{\lambda(\tau)\}}{d\tau}\right]^{-1}_{\tau=\tau_j^\pm} = \mathrm{Re}\left\{\frac{(2\lambda+p_1)e^{\lambda\tau}}{(q_1\lambda+q_2)\lambda}\right\}_{\tau=\tau_j^\pm} + \mathrm{Re}\left\{\frac{q_1}{(q_1\lambda+q_2)\lambda}\right\}_{\tau=\tau_j^\pm} - \mathrm{Re}\left\{\frac{\tau}{\lambda}\right\}_{\tau=\tau^\pm}\\
&= \mathrm{Re}\left\{\frac{(2\omega_\pm i+p_1)(\cos(\omega_\pm\tau_j^\pm)-i\sin(\omega_\pm\tau_j^\pm))}{(q_1\omega_\pm i+q_2)\omega_\pm i}\right\} + \mathrm{Re}\left\{\frac{q_1}{(q_1\omega_\pm i+q_2)\omega_\pm i}\right\}\\
&= \left\{\frac{2q_2\omega_\pm\cos(\omega_\pm\tau_j^\pm)+p_1q_2\sin(\omega_\pm\tau_j^\pm)-p_1q_1\omega_\pm\cos(\omega_\pm\tau_j^\pm)+2q_1\omega_\pm^2\sin(\omega_\pm\tau_j^\pm)}{(q_2^2+q_1^2\omega^2)\omega_\pm}\right\} - \left\{\frac{q_1^2}{(q_2^2+q_1^2\omega_\pm^2)}\right\}\\
&= \left\{\frac{(2q_2-p_1q_1)\omega\cos(\omega_\pm\tau_j^\pm)+(p_1q_2+2q_1\omega^2)\sin(\omega_\pm\tau_j^\pm)-q_1^2\omega_\pm}{(q_2^2+q_1^2\omega_\pm^2)\omega}\right\}\\
&= \frac{1}{q_2^2+q_1^2\omega^2}\left\{2\omega_\pm^2 + (p_1^2 - 2p_2 - q_1^2)\right\} = \frac{1}{q_2^2+q_1^2\omega^2}\left\{\pm\sqrt{\Delta}\right\},
\end{aligned}$$

where Δ is the discriminant of Eq. (40). Thus, if $\Delta \neq 0$, we have

$$\left[\frac{d\mathrm{Re}\{\lambda(\tau)\}}{d\tau}\right]_{\tau=\tau_j^+} = \left[\frac{d\mathrm{Re}\{\lambda(\tau)\}}{d\tau}\right]^{-1}_{\tau=\tau_j^+} = \frac{1}{q_2^2 + q_1^2\omega^2}\left\{\sqrt{\Delta}\right\} > 0$$

and

$$\left[\frac{d\mathrm{Re}\{\lambda(\tau)\}}{d\tau}\right]_{\tau=\tau_j^-} = \left[\frac{d\mathrm{Re}\{\lambda(\tau)\}}{d\tau}\right]^{-1}_{\tau=\tau_j^-} = -\frac{1}{q_2^2 + q_1^2\omega^2}\left\{\sqrt{\Delta}\right\} < 0,$$

which completes the proof. □

To apply these results to investigating stability of the trivial solution of the system (1) with a weak distribution kernel (32), we start by noting that for $\tau = 0$, all roots of (43) have negative real parts if and only if (H4) is satisfied, which has explicit form

$$\begin{cases} \alpha < \kappa - \beta, & \text{if } n \text{ is odd,} \\ \alpha < \kappa + |\beta|, & \text{if } n \text{ is even.} \end{cases} \tag{44}$$

It, therefore, follows that the trivial steady state of a ring neuron system (1) without delay in self-connection is asymptotically stable if and only if the conditions (44) are satisfied. To explore the effects of the self-connection delay on stability, we now check the hypotheses (H1–H3) by substituting p_1, p_2, q_1, and q_2. Substituting the expressions for these parameters from (37) into conditions $p_2^2 - q_2^2 > 0$ and $q_1^2 + 2p_1 - p_1^2 < 0$ of (H1), one finds

$$\alpha < \kappa + |\beta|, \tag{45}$$

and

$$|\alpha| < \kappa \quad \text{and} \quad \beta > -\frac{\gamma}{2}. \tag{46}$$

Similarly, the condition $p_2^2 - q_2^2 < 0$ in (H2) now takes an explicit form

$$\begin{cases} \alpha > |\kappa - \beta|, & \text{if } n \text{ is odd,} \\ \alpha > |\kappa \pm \beta|, & \text{if } n \text{ is even.} \end{cases} \tag{47}$$

Finally, the condition $p_2^2 - q_2^2 > 0$ in (H3) is the same as the condition (45), whereas conditions $q_1^2 + 2p_1 - p_1^2 > 0$, $\Phi > 0$ give (47) and

$$\begin{cases} |\alpha| > \kappa \text{ and } \beta < -\frac{\gamma}{2}, & \text{if } n \text{ is odd,} \\ |\alpha| > \kappa \text{ and } |\beta| < -\frac{\gamma}{2}, & \text{if } n \text{ is even.} \end{cases} \tag{48}$$

Using Lemmas 4 and 5, one can draw the following conclusions about the stability of the trivial steady state.

Theorem 9 *For the system* (1) *with weak gamma distributed delayed kernel* (32) *with* $p = 1$, *when n is even, and* $\tau_j^{\pm}$ *being defined in* (42), *the following results hold.*

(i) *The trivial steady state is unstable if* $|\beta| > \kappa - \alpha$.
(ii) *The trivial steady state is asymptotically stable if* $\alpha < \kappa + |\beta|$ *and* $|\alpha| < \kappa$.

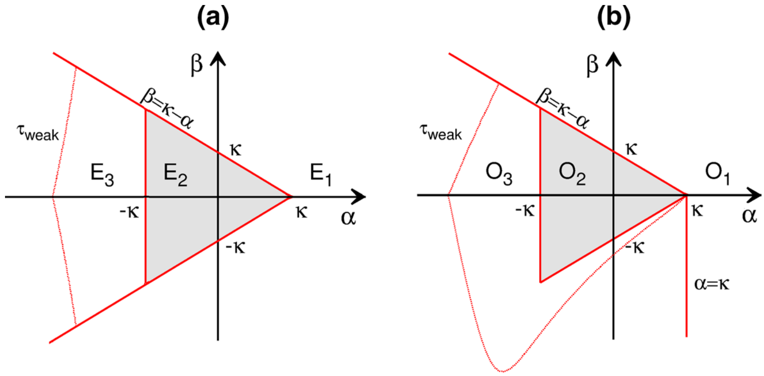

Fig. 8 Stability boundary of the trivial steady state of the system (1) for weak gamma distributed kernel with n even (**a**), or n odd (**b**). The trivial steady state is unstable in regions E_1/O_1, asymptotically stable in regions E_2/O_2 for any τ, and stable in regions E_3/O_3 for $\tau \in [0, \tau_{weak})$

(iii) *The trivial steady state is stable if* $\alpha < \kappa + |\beta|$, $\alpha > -\kappa$ *and* $\tau \in [0, \tau_{weak})$, *unstable if* $\tau > \tau_{weak}$, *and undergoes a Hopf bifurcation at* $\tau = \tau_{weak}$.

Theorem 10 *For the system* (1) *with weak gamma distributed delayed kernel* (32) *with* $p = 1$, *odd* n, *and* $\tau_j^{\pm}$ *being defined in* (42), *the following resuls hold.*

(i) *The trivial steady state is unstable if* $\beta > \kappa - \alpha$ *and* $\alpha > \kappa$.
(ii) *The trivial steady state is asymptotically stable if* $\alpha < \kappa + |\beta|$ *and* $|\alpha| < \kappa$.
(iii) *The trivial steady state is stable if* $\beta < \kappa - \alpha$ *and* $\alpha < \kappa$ *and* $\tau \in [0, \tau_{weak})$, *unstable if* $\tau > \tau_{weak}$, *and undergoes a Hopf bifurcation at* $\tau = \tau_{weak}$.

Figure 8 illustrates stability regions of the trivial steady state of the system (1) in the case of weak gamma distribution. The trivial steady state is stable inside shaded triangular regions E_2 and O_2 that are larger compared to the case of the delta distributed kernel. Similar to the case of the delta distribution kernel, the stability region extends to the left of the triangle and remains symmetric along α-axis for an even number of neurons, and becomes asymmetric for negative values of β for an odd number of neurons.

Theorem 11 *For the system* (1) *with weak gamma distribution kernel* (32) *with* $p = 1$, *when* n *is even, and* $\tau_j^{\pm}$ *being defined in* (42), *the following results hold.*

(i) *For* $\alpha < 0$, *the trivial steady state is asymptotically stable if* $|\beta| < \kappa - \alpha$ *and* $\tau < (\alpha - \kappa - \gamma)/(\alpha\gamma)$. *As* β *is increased (decreased) through the line* $|\beta| = \kappa - \alpha$, *the trivial equilibrium loses its stability through a steady-state bifurcation. Furthermore, the trivial steady state is stable if* $|\beta| < \kappa - \alpha$ *and* $\tau \in \big[(\alpha - \kappa - \gamma)/(\alpha\gamma), \tau_{weak}\big)$, *unstable for* $\tau > \tau_{weak}$, *and undergoes a Hopf bifurcation at* $\tau = \tau_{weak}$. *For* $\alpha < -\kappa$, *the trivial steady state is unstable independently of* β *for* $\tau > \tau_0 = \cos^{-1}(\kappa/\alpha)/\sqrt{\alpha^2 - \kappa^2}$.
(ii) *For* $0 \le \alpha \le \kappa$, *the trivial steady state is asymptotically stable if* $|\beta| < \kappa - \alpha$, *and loses its stability through a steady state bifurcation when* β *is increased (decreased) through the line* $|\beta| = \kappa - \alpha$, *becoming unstable for* $|\beta| > \kappa - \alpha$.

Theorem 12 *For the system* (1) *with weak gamma distribution kernel* (32) *with* $p = 1$, *when* n *is odd, and* $\tau_j^{\pm}$ *being defined in* (42), *the following results hold.*

(i) *For* $\alpha < -\kappa$ *and* $\beta > 0$, *the trivial steady state is asymptotically stable if* $\beta < \kappa - \alpha$ *and* $\tau < (\alpha - \kappa - \gamma)/(\alpha\gamma)$. *When* β *is increased, once it passes the value of* $\beta = \kappa - \alpha$, *the trivial steady state loses its stability via a steady-state bifurcation. The trivial steady state is stable if* $\beta < \kappa - \alpha$ *and* $\tau \in [(\alpha - \kappa - \gamma)/(\alpha\gamma), \tau_{weak})$, *unstable if* $\tau > \tau_{weak}$, *and undergoes a Hopf bifurcation at* $\tau = \tau_{weak}$. *For* $\alpha < 0$ *and* $\beta < 0$, *the trivial steady state is stable if* $\tau \in [0, \tau_{weak})$, *unstable if* $\tau > \tau_{weak}$, *and undergoes a a Hopf bifurcation at* $\tau = \tau_{weak}$. *For* $\alpha < -\kappa$, *the trivial steady state is unstable independent of* β *for* $\tau > \tau_0 = \cos^{-1}(\kappa/\alpha)/\sqrt{\alpha^2 - \kappa^2}$.

(ii) *For* $0 \leq \alpha \leq \kappa$ *and* $\beta > 0$, *the trivial steady state is asymptotically stable if* $\beta < \kappa - \alpha$, *and loses its stability via a steady-state bifurcation as* β *is increased through the line* $\beta = \kappa - \alpha$, *independently of the time delay* τ. *For* $0 < \alpha \leq \kappa$ *and* $\beta < 0$, *the trivial steady state is stable if* $\tau \in [0, \tau_{weak})$, *a Hopf bifurcation occurs at* $\tau = \tau_{weak}$.

Similar to the case of the general distribution kernel and delta distributed kernel, the stability boundary in (τ, β) plane is similar to Figs. 6 and 7 for n even and odd, respectively. Substituting the mean time delay $E = 1/\gamma$ into the condition $\tau < [(\kappa - \alpha)E - 1]/\alpha$ turns it into $\tau < (\alpha - \kappa - \gamma)/(\alpha\gamma)$ which determines the range of τ values, for which the trivial steady state is stable, and now it depends not only on α, but also on γ and κ.

5 Examples and numerical simulations

In order to illustrate our analytical findings, in this section we consider two specific examples when n is even, and when n is odd in (1) for the cases when the delay distribution kernel is taken as Dirac delta function and in the form of a weak gamma distribution. We shall use a traceDDE toolbox (Breda et al. 2006) to compute the characteristic roots and determine stability regions for the trivial steady state of the system (1). We will also perform direct numerical simulations of the fully nonlinear system using *dde23* suite in Matlab.

5.1 Example: even number of ring-coupled neurons

As an example, we consider the system (1) with the smallest even number of neurons, namely, $n = 2$, as shown schematically in Fig. 9.

Figure 10a–c show numerically computed stability regions for the trivial steady state of the system (1) with delta distributed kernel and $n = 2$ in the (α, β) plane, with colour representing $[-\max\{\text{Re}(\lambda)\}]$. It can been seen that the shape of the stability area is symmetric across α-axis in direct agreement with Theorem 5. As time delay τ is increased, the stability region becomes smaller while retaining a roughly quadrangular shaper. In Fig. 10d–f, the stability area is computed in the (τ, β) plane for several values of α. For negative values of α, the steady state undergoes both Hopf and steady-state bifurcations, as shown in Fig. 10d–e), as described by Theorems 3 and 7. Figure 10f

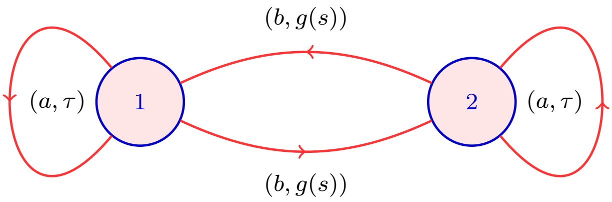

Fig. 9 A schematic sketch of two unidirectionally-coupled neurons with distributed delays and a discrete-delayed self-connection

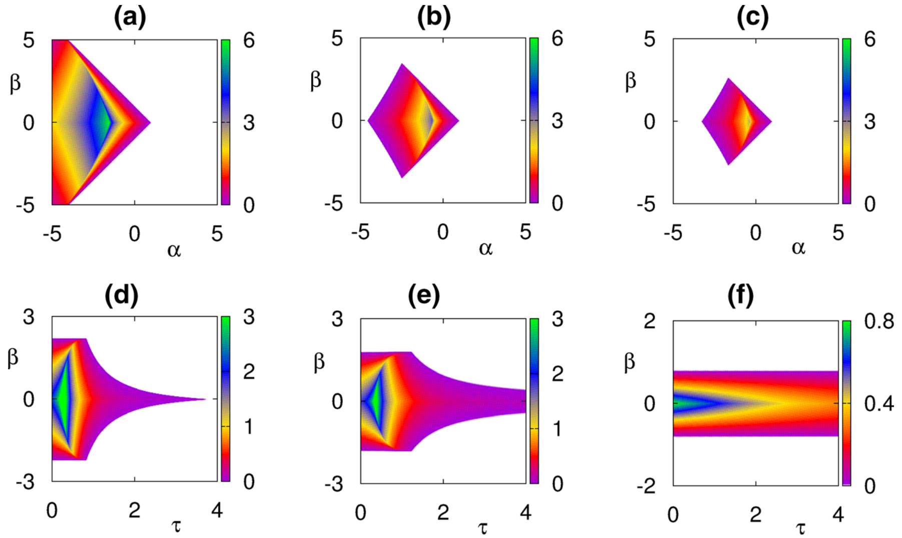

Fig. 10 Stability region for the trivial steady state of the system (1) with delta distributed kernel $g(s) = \delta(s)$ and $n = 2$. Colour code denotes $[-\max\{\text{Re}(\lambda)\}]$ for $\max\{\text{Re}(\lambda)\} \le 0$. **a–f** $\kappa = 1$. **a** $\tau = 0.2$. **b** $\tau = 0.4$. **c** $\tau = 0.6$. **d** $\alpha = -1.2$ $(\alpha < -\kappa)$. **e** $\alpha = -0.8$ $(-\kappa \le \alpha < 0)$. **f** $\alpha = 0.2$ $(0 \le \alpha \le \kappa)$ (color figure online)

corresponds to the case of positive values of $\alpha \in [0, \kappa]$, where the steady state can only undergo a steady-state bifurcation as per Remark 1.

In order to illustrate different types of dynamics that can be observed for various parameter combinations, we have also performed direct numerical simulations of the full nonlinear system (1) with $n = 2$ and a delta distributed kernel. Choosing the transfer function as $f(\cdot) = \tanh(\cdot)$, which implies that $f'(0) = 1$, we can rewrite system (1) for $n = 2$ and $g(s) = \delta(s)$ as follows,

$$\begin{aligned} \dot{u}_1(t) &= -\kappa u_1(t) + a\tanh(u_1(t-\tau)) + b\tanh(u_2(t)), \\ \dot{u}_2(t) &= -\kappa u_2(t) + a\tanh(u_2(t-\tau)) + b\tanh(u_1(t)). \end{aligned} \tag{49}$$

From Theorem 7(i) and (ii), it follows that whenever $\alpha < 0$, the trivial steady state is stable if $|\beta| < \kappa - \alpha$ and $\tau \in [-1/\alpha, \tau_{even})$. Here, we take $\kappa = 1$, $b = \pm 1$, $a = -0.8$, which gives the first critical value of the time delay, for which the trivial steady state loses its stability, as $\tau_{even} = 1.96$. In Figs. 11a and 12a, the trivial steady

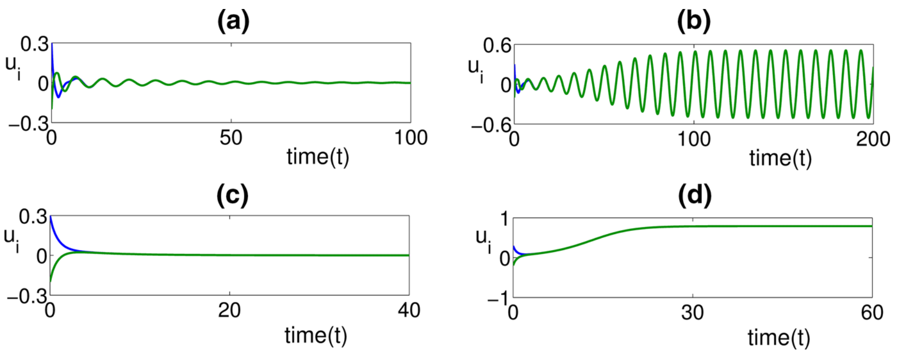

Fig. 11 **a**, **b** Numerical solution of the system (49) for $\alpha < 0$. Parameter values are $\kappa = 1, b = 1, a = -0.8$, and $\tau_{even} = 1.96$. **a** $0 < \tau = 1.8 < \tau_{even}$. **b** $\tau = 2.2 > \tau_{even}$. **c**, **d** Numerical solution of the system (49) in the case when $\alpha \geq 0$. Parameter values are $\kappa = 1, a = 0.2, \tau = 0.5$. **c** $b = 0.6$. **d** $b = 1$

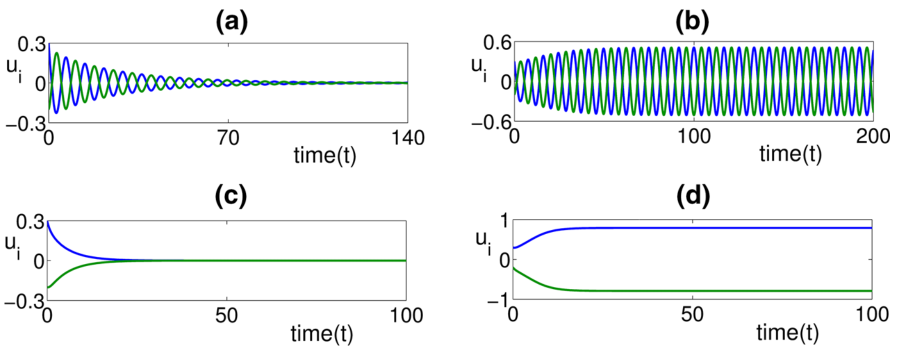

Fig. 12 **a**, **b** Numerical solution of the system (49) in the case when $\alpha < 0$. Parameter values are $\kappa = 1$, $b = -1, a = -0.8$ and $\tau_{even} = 1.96$. **a** $0 < \tau = 1.8 < \tau_{even}$. **b** $\tau = 2.2 > \tau_{even}$. **c**, **d** Numerical solution of the system (49) in the case when $\alpha \geq 0$. Parameter values are $\kappa = 1, a = 0.2, \tau = 0.5$. **c** $b = -0.6$. **d** $b = -1$

state is stable for $1.25 \leq \tau < 1.96$, and undergoes a Hopf bifurcation at $\tau_{even} = 1.96$, giving rise to a stable periodic solution, as shown in Figs. 11b and 12b. Note that when $\beta > 0$ and $\tau > \tau_{even}$, we observe an isochronal synchronous state illustrated in Fig. 11b, while for $\beta < 0$ and $\tau > \tau_{even}$, there is an anti-phase synchronous state presented in Fig. 12b.

The result from Theorem 7(iii) indicates that when $0 \leq \alpha \leq \kappa$, the trivial steady state is stable if $|\beta| < \kappa - \alpha$, which is satisfied for parameter values $\kappa = 1, a = 0.2$, $b = \pm 0.6$, and the corresponding solutions are shown in Figs. 11c and 12c. If $\beta > \beta_c$, where β_c satisfies $|\beta_c| = \kappa - \alpha$, the trivial steady state is a repeller, and there exists another stable non-trivial steady state, as illustrated in Figs. 11d and 12d.

Next, we consider the system (1) with a weak gamma distributed kernel. Following an idea of the linear chain trick (MacDonald 1978), we introduce two new variables

$$u_3(t) = \int_0^\infty \gamma e^{-\gamma s} u_1(t-s) ds,$$
$$u_4(t) = \int_0^\infty \gamma e^{-\gamma s} u_2(t-s) ds,$$

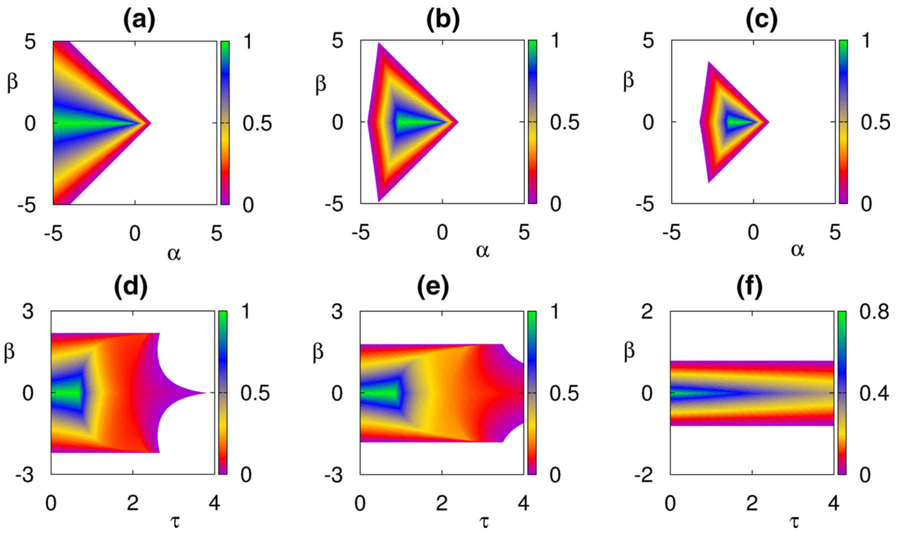

Fig. 13 Stability of the trivial steady state of the system (1) with weak gamma distributed kernel and $n = 2$. Colour code denotes $[-\max\{\mathrm{Re}(\lambda)\}]$ for $\max\{\mathrm{Re}(\lambda)\} \le 0$. **a–c** Stability region in (α, β), for parameters $\kappa = 1,\ \gamma = 1$. **a** $\tau = 0.2$. **b** $\tau = 0.4$. **c** $\tau = 0.6$. **d–f** Stability region in (τ, β), for parameters $\kappa = 1,\ \gamma = 1$. **d** $\alpha = -1.2\ (\alpha < -\kappa)$. **e** $\alpha = -0.8\ (-\kappa \le \alpha < 0)$. **f** $\alpha = 0.2\ (0 \le \alpha \le \kappa)$ (color figure online)

which allows us to equivalently rewrite the system 1 with $n = 2$ in the following way

$$\begin{aligned}
\dot{u}_1(t) &= -\kappa u_1(t) + a\tanh(u_1(t-\tau)) + b\tanh(u_4(t)),\\
\dot{u}_2(t) &= -\kappa u_2(t) + a\tanh(u_2(t-\tau)) + b\tanh(u_3(t)),\\
\dot{u}_3(t) &= \gamma u_1(t) - \gamma u_3(t),\\
\dot{u}_4(t) &= \gamma u_2(t) - \gamma u_4(t).
\end{aligned} \tag{50}$$

The stability region of the trivial steady state for the case of weak gamma distributed kernel in (α, β) parameter plane is shown in Fig. 13. This figure suggest that the stability region is larger compared to the case of delta distributed kernel for larger values of τ, but similarly to that distribution, for increasing τ, this stability region also shrinks while retaining symmetry with respect to α-axis, as shown in Fig. 13b, c. Similarly to the case of delta distributed kernel, in this case, there are three different boundary regions in (τ, β) parameter space depending on the values of α, and they are all symmetric with respect to the β-axis as plotted in Fig. 13d, f. This suggests that is it rather the absolute value of the coupling strength than its sign that determines stability of the trivial steady state, which for negative values of α can lose its stability via both a steady-state bifurcation, as well as a Hopf bifurcation, whereas for positive values of α only a steady-state bifurcation is possible.

Figure 14 illustrates the boundary of the stability region of the trivial steady state in β, τ and γ parameter space for the weak distribution kernel. If $\kappa = 1$ and $\alpha = -1$, the

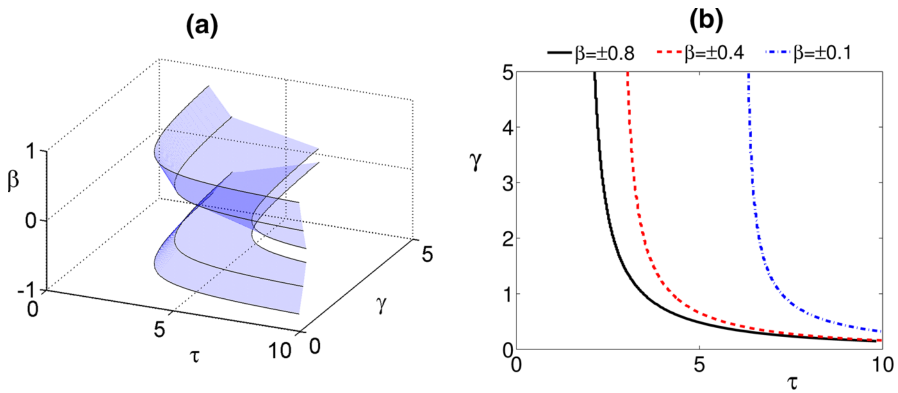

Fig. 14 Stability boundaries of the trivial steady state of the system (1) with weak gamma distributed kernel and $n = 2$. Parameter values are $\kappa = 1,\ \alpha = -1$. The trivial steady state is stable inside the region restricted by the boundaries in **a**, and to the left of the boundary curves in **b**

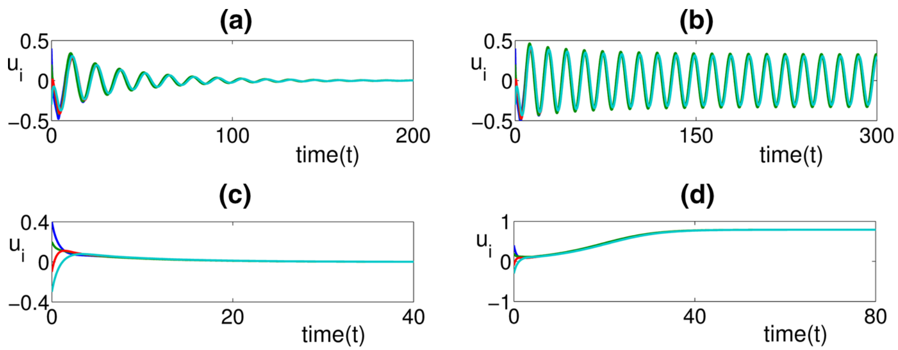

Fig. 15 **a**, **b** Numerical solution of the system (50) in the case when $\alpha < 0$. Parameter values are $\kappa = 1$, $b = 1$, $a = -0.8$, $\gamma = 1$, and $\tau_{weak} \approx 4.14$. **a** $0 < \tau = 3.8 < \tau_{weak}$. **b** $\tau = 4.3 > \tau_{weak}$. **c**, **d** Solution of the system (50) in the case when $\alpha \geq 0$. Parameter values are $\kappa = 1$, $a = 0.2$, $\gamma = 1$, $\tau = 0.5$. **c** $b = 0.6$. **d** $b = 1$

condition $-\kappa \leq \alpha < 0$ is satisfied, which means that the trivial steady state is stable inside the region bounded by symmetric surfaces shown in Fig. 14a, and unstable outside of this region. It can be observed in Fig. 14b that as the coupling strength β between the two neurons decreases, the region of stability of the trivial steady becomes larger.

From Theorem 11, when $\alpha < 0$, the trivial steady state is stable if $|\beta| < \kappa - \alpha$ and $\tau \in [(\alpha - \kappa - \gamma)/(\alpha\gamma), \tau_{weak})$. For parameter values $\kappa = 1$, $b = \pm 1$, $a = -0.8$, $\gamma = 1$, the first critical time delay in (42) is $\tau_{weak} \approx 4.14$. Thus, for $\tau \in [3.5, 4.14)$ the trivial steady state is stable, as shown in Figs. 15a and 16a, at $\tau_{weak} \approx 4.14$ a Hopf bifurcation occurs, and for $\tau_{weak} > 4.14$ periodic solutions are observed.

Moreover, similar to the delta distribution, Figs. 15b and 16b display isochronal and anti-phase states, respectively. If $\kappa = 1$, $a = 0.2$, $b = \pm 0.6$, then the conditions $0 \leq \alpha \leq \kappa$ and $|\beta| < \kappa - \alpha$ are satisfied, as required by Theorem 7(iii), thus ensuring the stability of the trivial steady state, as illustrated in Figs. 15c and 16c. If $\kappa = 1$,

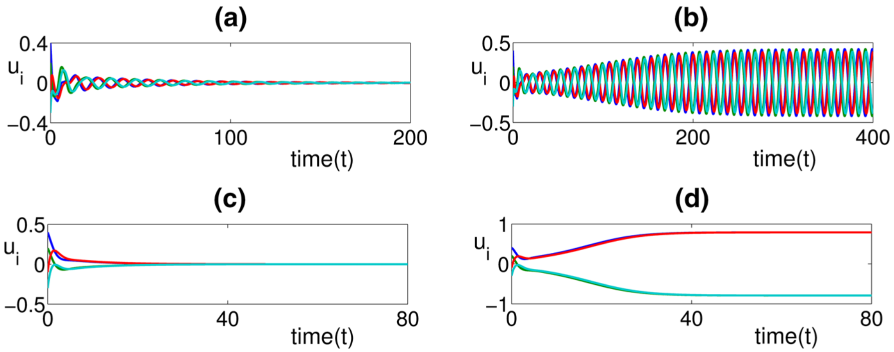

Fig. 16 **a**, **b** Numerical solution of the system (50) in the case when $\alpha < 0$. Parameter values are $\kappa = 1$, $b = -1$, $a = -0.8$, $\gamma = 1$ and $\tau_{weak} \approx 4.14$. **a** $0 < \tau = 3.8 < \tau_{weak}$. **b** $\tau = 4.3 > \tau_{weak}$. **c**, **d** Solution of the system (50) in the case when $\alpha \geq 0$. Parameter values are $\kappa = 1$, $a = 0.2$, $\gamma = 1$, $\tau = 0.5$. **c** $b = -0.6$. **d** $b = -1$

$a = 0.2$, $b = \pm 0.6$, and $\beta \geq \pm 0.8$, then the condition $|\beta| \geq \kappa - \alpha$ is satisfied, and the trivial steady state becomes unstable through a steady-state bifurcation, in which case the system (50) tends to one of its stable non-trivial steady states, as shown in Figs. 15d and 16d. One should note that it is possible for this system to simultaneously have multiple stable steady states for the same parameter values, and the solutions will approach one of them depending on initial conditions.

5.2 Example: odd number of ring-coupled neurons

For the second example, we consider three unidirectionally-coupled neurons with self-connections as shown in the diagrammatic sketch shown below in Fig. 17. If the distribution kernel is chosen as a delta function, i.e. $g(s) = \delta(s)$, the system (1) takes the form

$$\begin{aligned} \dot{u}_1(t) &= -\kappa u_1(t) + a \tanh(u_1(t-\tau)) + b \tanh(u_3(t)), \\ \dot{u}_2(t) &= -\kappa u_2(t) + a \tanh(u_2(t-\tau)) + b \tanh(u_2(t)), \\ \dot{u}_3(t) &= -\kappa u_3(t) + a \tanh(u_3(t-\tau)) + b \tanh(u_1(t)). \end{aligned} \tag{51}$$

Figure 18a, c show the stability region of the trivial steady state for delta distributed kernel $g(s) = \delta(s)$ in (α, β) parameter plane when $n = 3$. Similarly to the case of delta function with $n = 2$, the region of stability becomes smaller with increasing time delay τ, but unlike the case of the even number of neurons, here the region of stability is asymmetric with respect to α-axis.

Figure 18d, f illustrate stability boundaries of the trivial steady state in (τ, β) parameter plane for different values of α. In Fig. 18d, e, when $\alpha < 0$ and $\beta > 0$, similarly to the case when $n = 2$, the boundary of stability region consists of two different parts, which describe the trivial steady state losing its stability via a steady-state and a Hopf bifurcation, respectively. In contrast, for positive values of α and β, the trivial steady state can only undergo a steady-state bifurcation, as shown in Fig. 18f. Unlike the case of an even number of neurons, when $\beta < 0$, the trivial steady state can only lose its

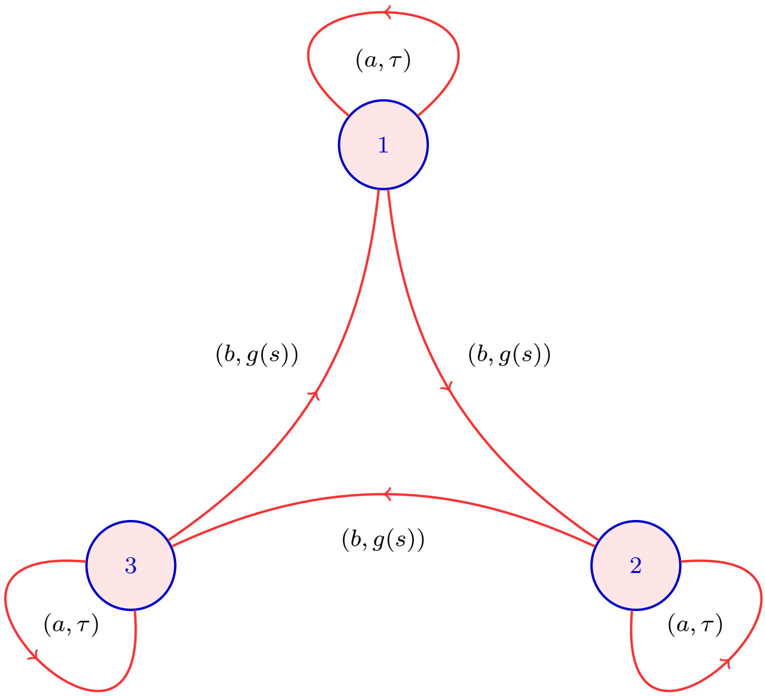

Fig. 17 A diagrammatic sketch of the unidirectionally coupled three neurons with distributed delays and a discrete-delayed self-connection

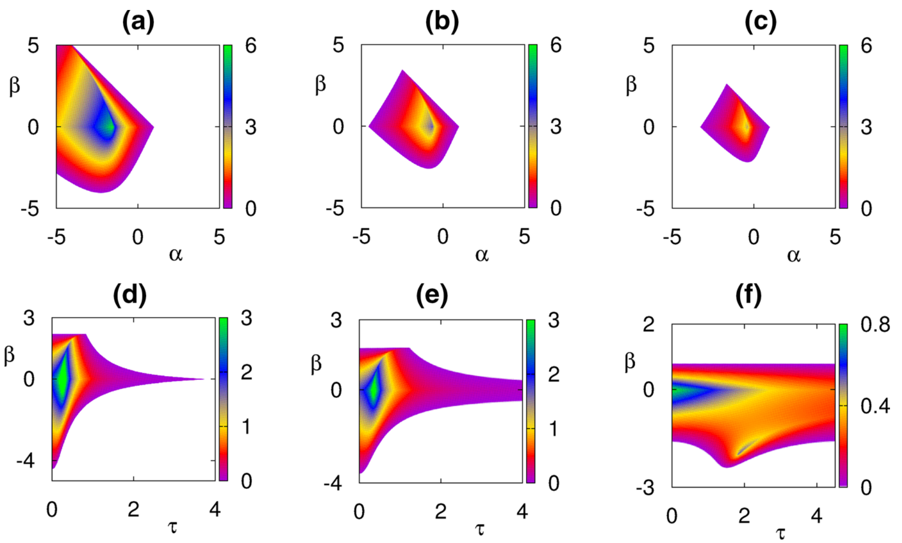

Fig. 18 Stability boundary of the trivial steady state of the system (1) with delta distributed kernel $g(s) = \delta(s)$, $n = 3$ and $\kappa = 1$. Colour code denotes $[-\max\{\text{Re}(\lambda)\}]$ for $\max\{\text{Re}(\lambda)\} \leq 0$. **a–c** Stability region in (α, β) parameter plane. Parameter values are **a** $\tau = 0.2$, **b** $\tau = 0.4$, **c** $\tau = 0.6$. **d–f** Stability region in (τ, β) parameter plane. Parameter values are **d** $\alpha = -1.2\,(\alpha < -\kappa)$. **e** $\alpha = -0.8\,(-\kappa \leq \alpha < 0)$. **f** $\alpha = 0.2\,(0 \leq \alpha \leq \kappa)$ (color figure online)

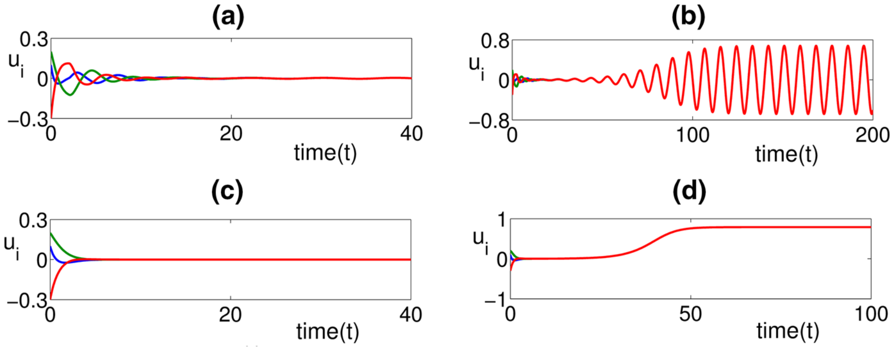

Fig. 19 **a**, **b** Numerical solution of the system (51) in the case when $\alpha < 0$. Parameter values are $\kappa = 1$, $b = 1$, $a = -0.8$ and $\tau_{odd} \approx 1.96$. **a** $0 < \tau = 1.8 < \tau_{odd}$. **b** $\tau = 2.2 > \tau_{odd}$. **c**, **d** Numerical solution of the system (51) in the case when $\alpha \geq 0$. Parameter values are $\kappa = 1$, $\tau = 0.5$, $a = 0.2$. **c** $b = 0.9$. **d** $b = 1.3$

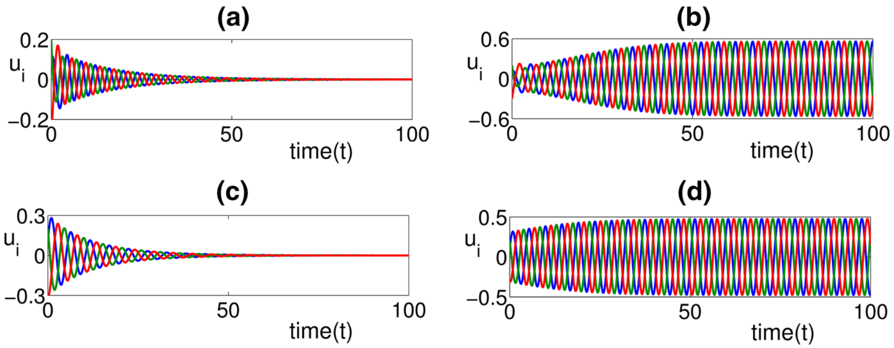

Fig. 20 **a**, **b** Numerical solution of the system (51) in the case when $\alpha < 0$. Parameter values are $\kappa = 1$, $b = -1$, $a = -0.8$ and $\tau_{odd} \approx 1.56$. **a** $0 < \tau = 1.3 < \tau_{odd}$. (b) $\tau = 1.8 > \tau_{odd}$. **c**, **d** Numerical solution of the system (51) in the case when $\alpha \geq 0$. Parameter values are $\kappa = 1$, $\tau = 0.5$, $a = 0.2$. **c** $b = -1.5$. **d** $b = -1.8$

stability via a Hopf bifurcation, resulting in asymmetry of the stability region with respect to α-axis.

From the analysis in Sect. 3 for an odd number of neurons, stability of the trivial steady state depends on whether the coupling strength β is positive or negative. For $\beta > 0$ the analysis is similar to that in the case of an even number of neurons. If $\alpha = af'(0) = -0.8 < 0$, $\beta = bf'(0) = 1 > 0$, $\kappa = 1$, the condition $\beta < \kappa - \alpha$ is satisfied, and from Eq. (27), we obtain $\tau_{odd} \approx 1.96$. This suggests that for $\tau \in [0, \tau_{odd})$ the trivial steady state is stable, as shown in Fig. 19a, and for $\tau > \tau_{odd}$ it is unstable, and the system displays synchronised periodic oscillations, as shown in Fig. 19b. In the case when $\kappa = 1$, $a = 0.2$, the condition $0 \leq \alpha \leq \kappa$ holds, and for $b = 0.9$, solutions tend to the trivial steady state, as illustrated in Fig. 19c, while for $b = 1$, the solutions converge to a non-trivial steady state, as shown in Fig. 19d.

Next, we consider negative values of β. If $\kappa = 1$, $b = -1$, $a = -0.8$, then $\tau_{odd} \approx 1.56$, and the trivial steady state is stable for $0 \leq \tau < \tau_{odd}$ and unstable for $\tau > \tau_{odd}$, with the system exhibiting a splay-state periodic solution in the latter case, as shown in Fig. 20a, b. A similar situation is observed when $\alpha \geq 0$, where fixing $\kappa = 1$, $a = 0.2$, we observe that solutions approach the trivial steady state for $b = -1.5$ (Fig. 20c), and for a more negative $b = -1.8$, they again exhibit splay-state periodic oscillations around the trivial steady state (Fig. 20d), indicating a difference from the case $n = 2$, where periodic solutions were synchronised.

Using the same linear chain trick as for $n = 2$, in the case of the weak gamma distributed kernel, we introduce the new variables

$$
\begin{aligned}
u_4(t) &= \int_0^\infty \gamma e^{-\gamma s} u_1(t-s)ds, \\
u_5(t) &= \int_0^\infty \gamma e^{-\gamma s} u_2(t-s)ds, \\
u_6(t) &= \int_0^\infty \gamma e^{-\gamma s} u_3(t-s)ds,
\end{aligned}
$$

and replace the system (1) with $n = 3$ by an equivalent six-dimensional system with only discrete time delays as follows,

$$
\begin{aligned}
\dot{u}_1(t) &= -\kappa u_1(t) + a \tanh(u_1(t-\tau)) + b \tanh(u_6(t)), \\
\dot{u}_2(t) &= -\kappa u_2(t) + a \tanh(u_2(t-\tau)) + b \tanh(u_5(t)), \\
\dot{u}_3(t) &= -\kappa u_3(t) + a \tanh(u_3(t-\tau)) + b \tanh(u_4(t)), \\
\dot{u}_4(t) &= \gamma u_1(t) - \gamma u_4(t), \\
\dot{u}_5(t) &= \gamma u_2(t) - \gamma u_5(t), \\
\dot{u}_6(t) &= \gamma u_3(t) - \gamma u_6(t).
\end{aligned}
\tag{52}
$$

Figure 21a, c show the stability region of the trivial steady state in (α, β) parameter plane for the weak gamma distributed delay kernel. Similarly to the case of $n = 2$, increasing the time delay τ reduces the size of the stability region, but now, for an odd number of neurons, it also loses its symmetry with respect to the α-axis. Figure 21d, f illustrate stability regions in (τ, β) plane for different values of α. One observes that changing α from negative to positive results in a trivial steady state undergo both steady-state and Hopf bifurcation for positive β, or only a steady-state bifurcation.

Figure 22 illustrates the stability region in the parameter space of β, τ, and γ for the weak gamma distributed kernel and $n = 3$. The steady state is stable between the two surfaces in Fig. 22a, and unstable everywhere else. Fig. 22b, c illustrate the stability region in (τ, γ) plane, suggesting that the stability area grows as the coupling strength $\beta > 0$ is decreased, or $\beta < 0$ is increased.

As can be seen in Figs. 23a and 24a, the trivial steady is stable for $\tau < \tau_{weak}$. As the value of the time delay τ exceeds its critical value $\tau = \tau_{weak}$, the trivial steady state loses its stability, giving rise to synchronised or splay-state oscillations shown in Figs. 23b and 24b, respectively. It is worth noting that depending on the sign of the coupling strength β, increasing it results in the solutions of the system moving away from the trivial steady state to either another non-trivial steady state for positive β, as shown in Fig. 23d, or to a periodic solution around the trivial steady state for negative β, as in Fig. 24d.

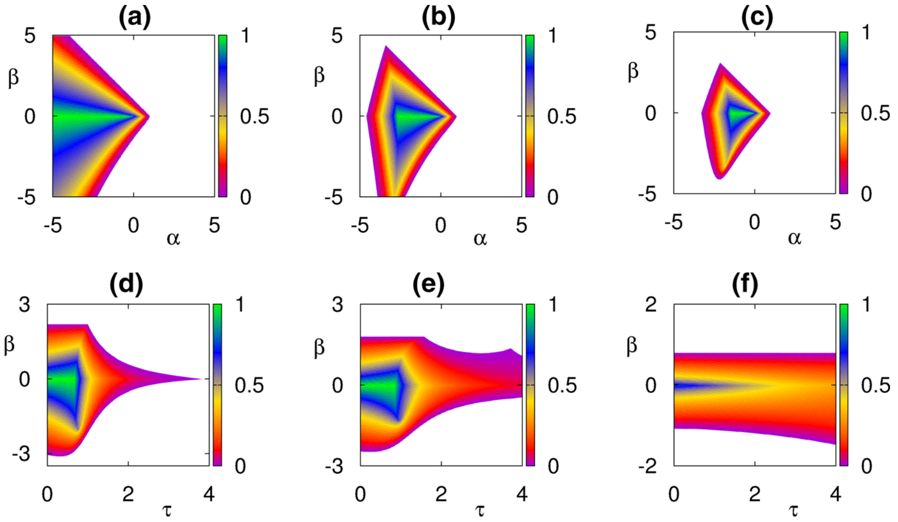

Fig. 21 Stability of the trivial steady state of the system (1) with weak gamma distributed kernel and $n = 3$. Colour code denotes $[-\max\{\mathrm{Re}(\lambda)\}]$ for $\max\{\mathrm{Re}(\lambda)\} \leq 0$. **a**–**c** Stability region in (α, β), for parameters $\kappa = 1,\ \gamma = 1$. **a** $\tau = 0.2$. **b** $\tau = 0.4$. **c** $\tau = 0.6$. **d**–**f** Stability region in (τ, β), for parameters $\kappa = 1,\ \gamma = 1$. **d** $\alpha = -1.2$ $(\alpha < -\kappa)$. **e** $\alpha = -0.8$ $(-\kappa \leq \alpha < 0)$. **f** $\alpha = 0.2$ $(0 \leq \alpha \leq \kappa)$ (color figure online)

6 Discussion

In this paper, we have analysed a unidirectionally-coupled ring neural network with n neurons with delay-distributed connections between neurons, and a discrete delayed self-feedback. We have analytically studied stability properties of the trivial steady state of the system in the case of a general distribution kernel, considering separately the cases of even and odd number of neurons in the system. Having identified subsets of stability regions, and in order to make further analytical progress and understand the dynamical behaviour of the system, we have focused on specific cases of delta and weak gamma distributed kernels.

In the case of Dirac delta distribution kernel, we have obtained analytical conditions for stability of the trivial steady state in terms of κ, α, β, and τ. For an even (odd) number of neurons, the stability region of the trivial solution reduces symmetrically (asymmetrically) along α-axis with increasing time delay τ in the $\alpha - \beta$ plane. In the case of weak gamma distribution, the stability region occupies a larger area in the $\alpha - \beta$ parameter plane compared to the case of the delta distributed kernel. In the $\tau - \beta$ parameter plane, changing the sign of the synaptic weight α can result in the trivial steady state to losing its stability via steady-state bifurcation, giving rise to a stable non-trivial steady state, and/or via a Hopf bifurcation giving rise to a stable periodic solution.

We have also performed direct numerical simulations that support and illustrate our analytical results. Choosing parameter values both inside and outside stability regions, we were able to further explore the dynamics of the system for both delta and weak gamma distributions, and both even and odd numbers of neurons in the network.

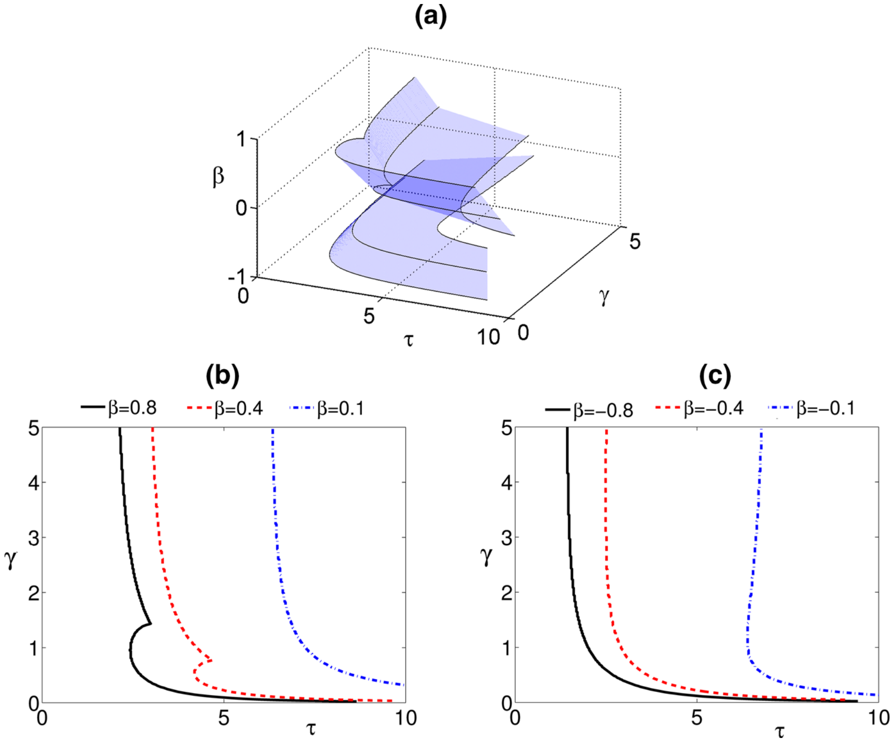

Fig. 22 Stability boundary for the trivial steady state of the system (1) with weak gamma distributed kernel and $n = 3$. Parameter values are $\kappa = 1,\ \alpha = -1$. The trivial steady state is stable inside the region restricted by the boundaries in **a**, and to the left of the boundary curves in **b**, **c**

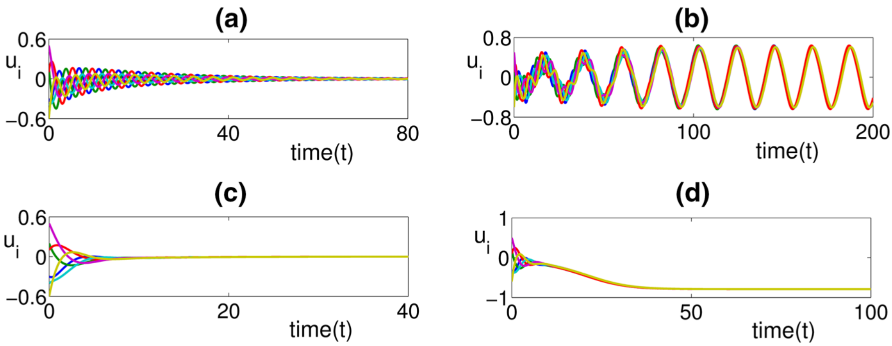

Fig. 23 **a**, **b** Numerical solution of the system (52) in the case when $\alpha < 0$. Parameter values are $\kappa = 1$, $b = 1.5$, $a = -0.8$, $\gamma = 1$ and $\tau_{weak} \approx 1.87$. **a** $0 < \tau = 1.5 < \tau_{weak}$. **b** $\tau = 4 > \tau_{weak}$. **c**, **d** Numerical solution of the system (52) in the case when $\alpha \geq 0$. Parameter values are $\kappa = 1$, $\gamma = 1$, $\tau = 0.5$, $a = 0.2$. **c** $b = 0.6$. **d** $b = 1$

We have observed isochronal synchronous, anti-phase synchronous and splay-state synchronous periodic oscillations when the time delay exceeds a certain critical value, and a trivial steady state loses its stability.

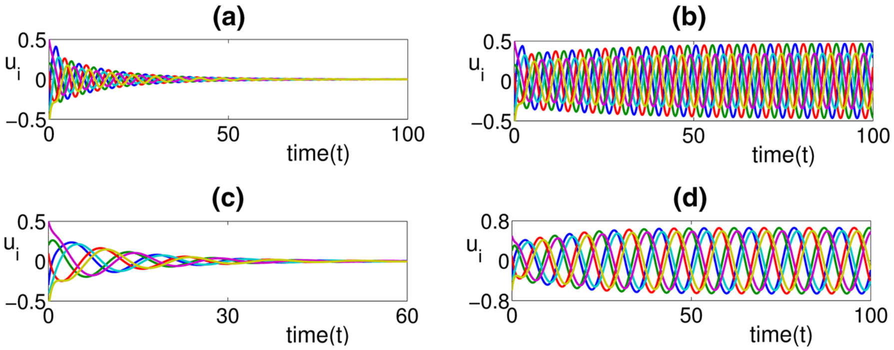

Fig. 24 **a**, **b** Numerical solution of the system (52) in the case when $\alpha < 0$. Parameter values are $\kappa = 1$, $b = -1$, $a = -0.8$, $\gamma = 1$ and $\tau_{weak} \approx 2.13$. **a** $0 < \tau = 1.8 < \tau_{weak}$. **b** $\tau = 2.2 > \tau_{weak}$. **c**, **d** Numerical solution of the system (52) in the case when $\alpha \geq 0$. Parameter values are $\kappa = 1$, $\gamma = 1$, $\tau = 0.5$, $a = 0.2$. **c** $b = -0.9$. **d** $b = -1.2$

There are several directions in which the work presented in this paper could be extended. One interesting possibility is to considering a similar architecture but with a bidirectional delay-distributed coupling between neurons, which would generalise an earlier work considered in Yuan and Campbell (2004), Campbell et al. (2005), Huang and Wu (2003) and Xu (2008). Another direction is to extend the work of Mao (2012) and Mao and Wang (2015) on low-dimensional neural subnetworks with discrete delay coupling to systems of multiple unidirectionally-coupled rings of neurons.

References

Ahmadkhanlou F, Adeli H (2005) Optimum cost design of reinforced concrete slabs using neural dynamics model. Eng Appl Artif Intell 18:65–72

Amari S, Cichocki A (1998) Adaptive blind signal processing-neural network approaches. Proc IEEE 86:2026–2048

Andersen P, Gross O, Lomo T, Sveen O (1969) Participation of inhibitory interneurons in the control of hippocampal cortical output. UCLA Forum Med Sci 11:415–465

Atay FM, Hutt A (2006) Neural fields with distributed transmission speeds and long-range feedback delays. SIAM J Appl Dyn Syst 5:670–698

Atiya AF, Baldi P (1989) Oscillations and synchronizations in neural networks: an exploration of the labeling hypothesis. Int J Neural Syst 1:103–124

Baldi P, Atiya AF (1994) How delays affect neural dynamics and learning. IEEE Trans Neural Netw 5:612–621

Bernard S, Bélair J, Mackey MC (2001) Sufficient conditions for stability of linear differential equations with distributed delay. Discrete Contin Dyn Syst B 1:233–256

Bi P, Hu Z (2012) Hopf bifurcation and stability for a neural network model with mixed delays. Appl Math Comput 218:6748–6761

Breda D, Maset S, Vermiglio R (2006) Pseudospectral approximation of eigenvalues of derivative operators with non-local boundary conditions. Appl Numer Math 56:318–331

Campbell SA (2007) Time delays in neural systems. In: Jirsa VK, McIntosh AR (eds) Handbook of brain connectivity. Springer, Berlin, pp 65–90

Campbell SA, Ruan S, Wolkowicz G, Wu J (1999) Stability and bifurcation of a simple neural network with multiple time delays. Fields Inst Commun 21:65–79

Campbell SA, Yuan Y, Bungay SD (2005) Equivariant Hopf bifurcation in a ring of identical cells with delayed coupling. Nonlinearity 18:2827

Canavier CC, Butera RJ, Dror RO, Baxter DA, Clark JW, Byrne JH (1997) Phase response characteristics of model neurons determine which patterns are expressed in a ring circuit model of gait generation. Biol Cybern 77:367–380

Cushing JM (1977) Integrodifferential equations and delay models in population dynamics. Lect Notes Biomath 20:501–594

Dror RO, Canavier CC, Butera RJ, Clark JW, Byrne JH (1999) A mathematical criterion based on phase response curves for stability in a ring of coupled oscillators. Biol Cybern 80:11–23

Du Y, Xu R, Liu Q (2013) Stability and bifurcation analysis for a neural network model with discrete and distributed delays. Math Methods Appl Sci 36:49–59

Eccles JC, Ito M, Szentágothai J (1967) Cerebellum as neuronal machine. Springer, New York

Erneux T (2009) Applied delay differential equations. Springer, New York

Feng C (2014) Oscillatory behavior on a three-node neural network model with discrete and distributed delays. Adv Artif Neural Syst 1:1–9

Feng P (2010) Dynamics of a segmentation clock model with discrete and distributed delays. Int J Biomath 3:399–416

Forti M, Tesi A (1995) New conditions for global stability of neural networks with application to linear and quadratic programming problems. IEEE Trans Circuits Syst I(42):354–366

Gjurchinovski A, Urumov V (2010) Variable-delay feedback control of unstable steady states in retarded time-delayed systems. Phys Rev E 81:016209

Gjurchinovski A, Zakharova A, Schöll E (2014) Amplitude death in oscillator networks with variable-delay coupling. Phys Rev E 89:032915

Gjurchinovski A, Schöll E, Zakharova A (2017) Control of amplitude chimeras by time delay in oscillator networks. Phys Rev E 95:042218

Gopalsamy K (2013) Stability and oscillations in delay differential equations of population dynamics. Springer, Berlin, p 74

Gopalsamy K, Leung I (1996) Delay induced periodicity in a neural netlet of excitation and inhibition. Phys D 89:395–426

Gourley SA, So JW-H (2003) Extinction and wavefront propagation in a reaction-diffusion model of a structured population with distributed maturation delay. Proc R Soc Edinb 133:527–548

Gu K, Kharitonov L, Chen L (2003) Stability of time-delay system. Birkhäuser, Boston

Guo S, Huang L (2003) Hopf bifurcating periodic orbits in a ring of neurons with delays. Phys D 183:19–44

Han Y, Song Y (2012) Stability and Hopf bifurcation in a three-neuron unidirectional ring with distributed delays. Nonlinear Dyn 69:357–370

Hassard BD, Kazarino ND, Wan Y-H (1981) Theory and applications of Hopf bifurcation. CUP Arch 41:0076–0552

Hopfield JJ (1984) Neurons with graded response have collective computational properties like those of two-state neurons. Proc Natl Acad Sci USA 81:3088–3092

Huang L, Wu J (2003) Nonlinear waves in networks of neurons with delayed feedback: pattern formation and continuation. SIAM J Math Anal 34:836–860

Hutt A, Zhang L (2013) Distributed nonlocal feedback delays may destabilize fronts in neural fields, distributed transmission delays do not. J Math Neurosci 3:9

Jiang J, Song Y (2014) Bifurcation analysis and spatiotemporal patterns of nonlinear oscillations in a ring lattice of identical neurons with delayed coupling. Abstr Appl Anal 2014:368652

Karaoğlu E, Yılmaz E, Merdan H (2016) Stability and bifurcation analysis of two-neuron network with discrete and distributed delays. Neurocomputing 182:102–110

Kaslik E, Balint S (2009) Complex and chaotic dynamics in a discrete-time-delayed Hopfield neural network with ring architecture. Neural Netw 22:1411–1418

Khokhlova T, Kipnis M (2012) Numerical and qualitative stability analysis of ring and linear neural networks with a large number of neurons. Int J Pure Appl Math 76:403–419

Kuang Y (1993) Delay differential equations with applications in population dynamics. Academic Press, New York

Kyrychko YN, Blyuss KB, Schöll E (2011) Amplitude death in systems of coupled oscillators with distributed-delay coupling. Eur Phys J B 84:307–315

Kyrychko YN, Blyuss KB, Schöll E (2013) Amplitude and phase dynamics in oscillators with distributed-delay coupling. Philos Trans R Soc A 371:20120466

Kyrychko YN, Blyuss KB, Schöll E (2014) Synchronization of networks of oscillators with distributed delay coupling. Chaos 24:043117

Lai Q, Hu B, Guan Z-H, Li T, Zheng D-F, Wu Y-H (2016) Multistability and bifurcation in a delayed neural network. Neurocomputing 207:785–792

Li X, Hu G (2011) Stability and Hopf bifurcation on a neuron network with discrete and distributed delays. Appl Math Sci 5:2077–2084

Liao X, Wong K-W, Wu Z (2001) Hopf bifurcation and stability of periodic solutions for van der pol equation with distributed delay. Nonlinear Dyn 26:23–44

MacDonald N (1978) Time lags in biological systems. Springer, New York

Mao X (2012) Stability and Hopf bifurcation analysis of a pair of three-neuron loops with time delays. Nonlinear Dyn 68:151–159

Mao X, Wang Z (2015) Stability switches and bifurcation in a system of four coupled neural networks with multiple time delays. Nonlinear Dyn 82:1551–1567

Marcus CM, Westervelt RM (1989) Stability of analog neural networks with delay. Phys Rev A 39:347–359

May RM (1973) Time-delay versus stability in population models with two and three trophic level. Ecology 54:315–325

Mitra C, Ambika G, Banerjee S (2014) Dynamical behaviors in time-delay systems with delayed feedback and digitized coupling. Chaos 69:188–200

Pakdaman K, Grotta-Ragazzo C, Malta CP (1998) Transient regime duration in continuous-time neural networks with delay. Phys Rev E 58:3623–3627

Plaza J, Plaza A, Perez R, Martinez P (2009) On the use of small training sets for neural network-based characterization of mixed pixels in remotely sensed hyperspectral images. Pattern Recogn 42:3032–3045

Rahman B, Blyuss KB, Kyrychko YN (2015) Dynamics of neural systems with discrete and distributed time delays. SIAM J Appl Dyn Syst 14:2069–2095

Rahman B, Blyuss KB, Kyrychko YN (2017a) Aging transition in systems of oscillators with global distributed-delay coupling. Phys Rev E 96:032203

Rahman B, Kyrychko YN, Blyuss KB (2017b) Dynamics of neural systems with time delays. University of Sussex, Brighton

Ruan S, Filfil RS (2004) Dynamics of a two-neuron system with discrete and distributed delays. Phys D 191:323–342

Shayer LP, Campbell SA (2000) Stability, bifurcation, and multistability in a system of two coupled neurons with multiple time delays. SIAM J Appl Math 61:673–700

Song Y, Makarov VA, Velarde MG (2009) Stability switches, oscillatory multistability, and spatiotemporal patterns of nonlinear oscillations in recurrently delay-coupled neural networks. Biol Cybern 101:147–167

Stépán G (1989) Retarded dynamical systems: stability and characteristic functions. Longman Press, London

Szentágothai J (1975) The ‘module-concept’ in cerebral cortex architecture. Brain Res 95:475–496

Wang H, Wang J (2015) Hopf-pitchfork bifurcation in a two-neuron system with discrete and distributed delays. Math Methods Appl Sci 38:4967–4981

Williams CRS, Sorrentino F, Murphy TE, Roy R (2013) Synchronization states and multistability in a ring of periodic oscillators: experimentally variable coupling delays. Chaos Interdiscip J Nonlinear Sci 23:043117

Xie X, Hahnloser RHR, Seung HS (2002) Double-ring network model of the head-direction system. Phys Rev E 66:041902

Xu X (2008) Complicated dynamics of a ring neural network with time delays. J Phys A 41:035102

Xu C, Li P (2019) Influence of leakage delay on almost periodic solutions for BAM neural networks. IEEE Access 7:129741–129757

Xu W, Cao J (2014) Bifurcation analysis in a class of neural network models with discrete and distributed delays. In: Control conference (CCC), 33rd Chinese, IEEE, pp 6019–6024

Xu W, Cao J, Xiao M (2014) The stability and bifurcation analysis in high dimensional neural networks with discrete and distributed delays. In: 2014 international joint conference on neural networks (IJCNN), IEEE, pp 3739–3744

Xu C, Liao M, Li P, Guo Y (2019a) Bifurcation analysis for simplified five-neuron bidirectional associative memory neural networks with four delays. Neural Process Lett 361:1–27

Xu C, Liao M, Li P, Guo Y, Xiao Q, Yuan S (2019b) Influence of multiple time delays on bifurcation of fractional-order neural networks. Appl Math Comput 361:565–582

Xu C, Liao M, Li P, Guo Y, Yuan S (2019c) Joint influence of leakage delays and proportional delays on almost periodic solutions for FCNNs. Iran J Fuzzy Syst 17:1804–4433

Yuan Y, Campbell SA (2004) Stability and synchronization of a ring of identical cells with delayed coupling. J Dyn Differ Equ 16:709–744
Yuan S, Li X (2010) Stability and bifurcation analysis of an annular delayed neural network with self-connection. Neurocomputing 73:2905–2912
Zakharova A, Schneider I, Kyrychko YN, Blyuss KB, Koseska A, Fiedler B, Schöll E (2013) Time delay control of symmetry-breaking primary and secondary oscillation death. Europhys Lett 104:50004
Zakharova A, Semenova N, Anishchenko VS, Schöll E (2017) Time-delayed feedback control of coherence resonance chimeras. Chaos 27:114320
Zeng Z, Huang DS, Wang Z (2008) Pattern memory analysis based on stability theory of cellular neural networks. Appl Math Model 32:112–121
Zhao H (2004) Global asymptotic stability of Hopfield neural network involving distributed delays. Neural Netw 17:47–53
Zhou X, Wu Y, Li Y, Yao X (2009) Stability and Hopf bifurcation analysis on a two-neuron network with discrete and distributed delays. Chaos Solitons Fractals 40:1493–1505
Zhou X, Jiang M, Cai X (2011) Hopf bifurcation analysis for the van der Pol equation with discrete and distributed delays. Discrete Dyn Nat Soc. https://doi.org/10.1155/2011/569141
Zhu H, Huang L (2007) Stability and bifurcation in a tri-neuron network model with discrete and distributed delays. Appl Math Comput 188:1742–1756